


1-1-2021

The Probiotic Effect Of Clostridium Cochlearium Is Associated With Significant Change In Short-Chain Fatty Acid Metabolism And Gut Microbiota

Qing Ai
Wayne State University

Follow this and additional works at: https://digitalcommons.wayne.edu/oa_dissertations

 Part of the [Food Science Commons](#), [Microbiology Commons](#), and the [Nutrition Commons](#)

Recommended Citation

Ai, Qing, "The Probiotic Effect Of Clostridium Cochlearium Is Associated With Significant Change In Short-Chain Fatty Acid Metabolism And Gut Microbiota" (2021). *Wayne State University Dissertations*. 3434.
https://digitalcommons.wayne.edu/oa_dissertations/3434

This Open Access Dissertation is brought to you for free and open access by DigitalCommons@WayneState. It has been accepted for inclusion in Wayne State University Dissertations by an authorized administrator of DigitalCommons@WayneState.

**THE PROBIOTIC EFFECT OF *CLOSTRIDIUM COCHLEARIUM* IS ASSOCIATED
WITH SIGNIFICANT CHANGE IN SHORT-CHAIN FATTY ACID METABOLISM
AND GUT MICROBIOTA**

by

QING AI

DISSERTATION

Submitted to the Graduate School

of Wayne State University,

Detroit, Michigan

in partial fulfillment of the requirements

for the degree of

DOCTOR OF PHILOSOPHY

2021

MAJOR: NUTRITION AND FOOD SCIENCE

Approved By:

Advisor

Date

DEDICATION

This dissertation is dedicated to my beloved family, Qishuang Ai and Xiujiang Shen, for their love and support throughout my life.

ACKNOWLEDGMENTS

First, I would like to express my sincere gratitude to my advisor, Dr. Kequan Zhou, for mentoring me. I would like to thank him for his endless encouragement and patience. His constant support and advice are priceless for both my research and career. In addition to my advisor, I am grateful to Dr. Kai-Lin Jen, Dr. Ahmad Heydari, and Dr. Deborah Ellis for serving on my graduate committee. I would like to thank them for their valuable comments and advice on my projects and dissertation. My special thanks also go to Dr. Yifan Zhang's lab, Dr. Ahmad Heydari's lab, Dr. Diane Cress's lab, Dr. Kezhong Zhang's lab, and Dr. James Granneman's Lab. I appreciate their kindness in providing equipment and crucial help with my experiments. I also would like to express my gratitude to my past and present colleagues in Dr. Zhou's lab: Dr. Shi Sun, Dr. Kai Nie, Dr. Jiangqi Tang, Dr. Fei Yang, Wenjun Zhu, and Paba Edirisuriya. I will never forget those days we worked together to do experiments and hung out to eat delicious food. Finally, I would like to thank the University of Michigan Microbial Systems Molecular Biology Laboratory, which supported us for 16s rRNA sequencing running.

TABLE OF CONTENTS

DEDICATION	ii
ACKNOWLEDGMENTS	iii
LIST OF TABLES	vi
LIST OF FIGURES	vii
CHAPTER 1. INTRODUCTION	1
Obesity	1
Gut microbiota.....	2
Probiotics and short-chain fatty acids	4
<i>Clostridium cochlearium</i>	5
Specific aims	6
CHAPTER 2. DETERMINE THE EFFECT OF <i>C. COCHLERIUM</i> SUPPLEMENTATION ON A DIO MOUSE MODEL	7
Methods.....	7
Bacterial preparation.....	7
Experimental animals	8
Fecal energy analysis.....	9
Glucose homeostasis.....	9
Metabolic study and body composition analysis (BCA)	10
Results	12
Discussion	14
CHAPTER 3. DETERMINE THE EFFECT OF DIETARY <i>C. COCHLERIUM</i> TREATMENT ON GUT MICROBIOME PROFILE VIA 16S rRNA GENE SEQUENCING	18
Methods.....	18
16S rRNA-amplicon sequencing of gut microbiota	18

Statistical analysis.....	19
Results	20
Discussion	22
CHAPTER 4. DETERMINE THE POTENTIAL MECHANISM BASED ON GUT MICROBIOME.....	30
Methods	30
Functional gene analysis.....	30
Short-chain fatty acids measurement.....	31
RNA extraction.....	31
Reverse transcription-quantitative polymerase chain reaction (RT-PCR)	32
Real-time quantitative polymerase chain reaction (qPCR/real-time PCR)	32
Statistical analysis.....	32
Results	33
Discussion	37
Conclusion.....	41
Future direction	43
TABLES AND FIGURES	45
REFERENCES	80
ABSTRACT.....	98
AUTOBIOGRAPHICAL STATEMENT.....	100

LIST OF TABLES

Table 1. Nutrient composition and caloric content of the Low-fat Diet (LF) and the High-fat Diet (HF) used in the experiment	45
Table 2. Biometrics results in the LF, HF and CC groups at 16 weeks	46
Table 3. Blood biochemistry results in the LF, HF and CC groups at 16 weeks	47
Table 4. Energy balance results in the LF, HF and CC groups.....	48
Table 5. Metabolic results in the LF, HF and CC groups at 16 weeks	49
Table 6. Relative abundance of phylum classification in the HF and CC groups	50
Table 7. Primers for real-time PCR	51
Table 8. SCFAs-related predicted enzymes between the HF and CC groups.....	52
Table 9. Correlation between body weight and SCFAs-related predicted enzymes.....	53
Table 10. SCFAs-related predicted pathways between the HF and CC groups	54
Table 11. Correlation between body weight and SCFAs-related predicted pathways.....	55
Table 12. SCFAs concentration in intestinal content between the HF and CC groups.....	56

LIST OF FIGURES

Figure 1. Average percentage body weight gain over a 16-week period.....	57
Figure 2. Average fasting blood glucose tested every 4-week period	58
Figure 3. Average blood glucose measurement for oral glucose tolerance test over a 120-min period	59
Figure 4. Average AUC calculated from OGTT levels from Figure 3	60
Figure 5. Relative abundance of microbiota at Phylum level between the HF and CC groups	61
Figure 6. Pielou's evenness in alpha diversity between the HF and CC groups	62
Figure 7. Shannon diversity index in alpha diversity between the HF and CC groups	63
Figure 8. Faith's phylogenetic diversity (PD) in alpha diversity between the HF and CC groups.....	64
Figure 9. Unweighted Unifrac PCoA in beta diversity between the HF and CC groups	65
Figure 10. Weighted Unifrac PCoA in beta diversity between the HF and CC groups	66
Figure 11. Bray-Curtis PCoA in beta diversity between the HF and CC groups	67
Figure 12. Jaccard PCoA in beta diversity between the HF and CC groups	68
Figure 13. Biomarkers found by LEfSe results between the HF and CC groups.....	69
Figure 14. Cladograms of LEfSe results between the HF and CC groups	70
Figure 15. Intestinal <i>ffar2</i> relative gene expression	71
Figure 16. Intestinal <i>ffar3</i> relative gene expression	72
Figure 17. Intestinal <i>HCAR2</i> relative gene expression	73
Figure 18. Intestinal <i>SLC16A1</i> relative gene expression	74
Figure 19. Intestinal <i>SLC5A8</i> relative gene expression	75
Figure 20. Liver <i>ffar2</i> relative gene expression	76
Figure 21. Liver <i>ffar3</i> relative gene expression	77
Figure 22. Liver <i>HCAR2</i> relative gene expression	78

Figure 23. Butyrate synthesis pathways [160]	79
---	----

CHAPTER 1. INTRODUCTION

Obesity

Obesity among adults, defined as a body mass index (BMI) of 30 kg/m² or greater, has become a global pandemic. The prevalence of obesity has been increasing drastically around the world. In 2016, over 650 million adults were living with obesity, which is approximately 13% of adults across the globe [1]. According to the Centers for Disease Control and Prevention (CDC), the age-adjusted prevalence of obesity among adults significantly increased from 30.5% to 42.4% in the period from 1999 to 2018 in the United States [2]. Obesity is generally caused by an imbalance between energy intake and expenditure. High-fat diet-induced obesity is one of the common causes of obesity [3]. Diets that have over 30% of calorie intake from fat can easily contribute to obesity [4], and most Americans consume a diet with approximately 36% dietary fat [5].

Obesity increases the risks of various chronic diseases, including diabetes, hypertension, and cardiovascular disease (CVD) [6]. It has been considered as a vital risk factor for type 2 diabetes mellitus (T2DM), resulting in insulin resistance and consequently triggering the β -cell dysfunction [7, 8]. Studies have shown that over 80% of T2DM patients are overweight or obese, while approximately 50% of those have BMI over 30 kg/m² [9, 10]. Hypertension has also been associated with obesity mainly by increasing leptin levels, sympathetic nervous system activities, and renal sodium reabsorption activity [11]. It has been found that 60-70% of adults with hypertension are attributed to adiposity [12]. Cardiovascular disease has been proven as another obesity-associated comorbidity. Obesity heightens the risks of CVD due to the increase of cholesterol deposition through blood vessels [13]. Increasing obesity has also been associated with shortening of life expectancy between 0.2 and 11.7 years [14, 15].

Due to these adverse impacts, it is crucial to develop strategies for the prevention and treatment of obesity. Searching for methods to modify energy balance, which can also be influenced by biological, and behavioral, and environmental factors, has become a major approach that researchers are focusing on [16]. To reverse the occurrence of obesity, diet control, and physical exercise have been evaluated as potential approaches. A meta-analysis study by Andela et al. observed that reduced-energy diet (≤ 800 kcal/day) interventions resulted in an average weight loss of 10.1 kg ($P < 0.001$) lasting 3 to 20 weeks and maintaining a weight loss of 5.3 kg ($P < 0.001$) at follow-up (5 - 14.5 months) [17]. Isolated physical activity intervention improved body composition but is not an effective approach for confronting obesity [18]. Aerobic exercise interventions without calorie restriction showed a weight loss of 1.6 kg from 6-month programs and 1.7 kg from 12-month programs [19]. However, a combination of physical exercise and diet intervention has yielded better results than physical- or diet-only intervention [20]. A meta-analysis study by Johns et al. concluded that the combined physical and diet interventions yielded a similar short-term (3-6 months) weight loss and an increased weight loss during the long term (12-18 months) compared to the diet-only interventions [21].

Gut microbiota

The human gut microbiome is a complex and dynamic ecosystem colonized by approximately 10^{14} microbes, and microbes are symbiotic with the host [22, 23]. The initial colonization of microbes in the intestine is immediate at birth from maternal and environmental exposures, which becomes stable and complex by 2.5 years of age [24]. Although the gut microbiome community is stable in most cases, the composition can be shifted by external factors, including antibiotics overuse and diet modification [25, 26]. The use of antibiotics significantly disturbs the intestinal community, which may take four weeks or even longer to again resemble

the pre-treatment gut composition [27]. With antibiotics overuse, the risk of harboring antibiotic-resistant pathogens increases drastically [25]. Furthermore, diet is another crucial factor that significantly influences the intestinal community. An animal study conducted by Zhang et al. suggested that 57% of total composition changes in mouse intestines can be explained by high-fat diet modification, whereas genetic factors only account for 12% of the variations [28]. In addition, Arumugam et al. analyzed the fecal metagenomes of individuals and clustered the microbiome into three variants or enterotypes, including *Bacteroides*, *Prevotella*, and *Ruminococcus* [29]. Wu et al. further showed an association between these enterotypes and long-term dietary patterns, in which the *Bacteroides*-enriched enterotype was linked to a protein- and animal fats-based diet, while the *Prevotella*-enriched enterotype was related to dietary carbohydrates [30]. Currently, increasing experiments on humans and animal models have provided evidence suggesting a solid association between the gut microbiome and obesity [27, 31-33]. Studies have consistently indicated the linkage between obesity and an increased abundance of Firmicutes with a higher Firmicutes to Bacteroidetes ratio in the human gut [23, 34]. A potential mechanism could be due to the fact that Firmicutes are more effective in absorbing energy than Bacteroidetes do [35]. Animal studies also suggested that the gut microbiota of lean mice contained a 50% lower abundance of Firmicutes with an elevated abundance of Bacteroidetes compared to obese siblings [36, 37]. Turnbaugh et al. further indicated that more energy from diets was extracted by the gut microbiome of obese mice than that of lean mice [38]. Furthermore, Germ-free (GF) mice studies and fecal transplant studies have repeatedly shown the gut microbial influences on energy balance, specifically, energy consumption from food and energy storage in the host [38-40], suggesting the potential of probiotic interventions could be used to manage obesity [41-43].

Probiotics and short-chain fatty acids

Probiotics are live microorganisms that may directly modify the gut microbiome composition for positive health effects [44, 45]. *Lactobacillus* and *Bifidobacterium* species have been widely reviewed and used as probiotics in animal and human subjects, which are associated with relieving various types of diarrhea, such as antibiotic-induced, and rotavirus infection-induced diarrhea, improving inflammatory bowel disease (IBD) symptoms, and lowering the cholesterol synthesis [46, 47]. Once probiotics survive and colonize in the gut, specific species could produce antimicrobial substances, mediators, or metabolites, such as bacteriocins and short-chain fatty acids (SCFAs) [45]. These substances can inhibit other microorganisms from enumeration or colonization [48]; they can also compete against other gut microbes for receptors and binding sites [49]. For instance, *Lactobacillus johnsonii* La1 has been reported to effectively compete with enteropathogens because they both share the same carbohydrate-binding specificities in the intestine [50]. Likewise, certain metabolites produced by *Lactobacillus acidophilus*, including acidolin, acidophilin, and lactocidin, have been shown to inhibit the growth of food pathogens such as *Bacillus*, *Salmonella*, *E. coli*, and *Staphylococcus* [51, 52]. These mediators and metabolites produced by probiotics not only enhance the epithelial barrier and increased adhesion to the intestinal mucosa but also improve insulin sensitivity and the immune system, and influence energy intake [44, 53, 54]. SCFAs, which include formate, acetate, propionate, and butyrate, are major end products of the probiotic fermentation of non-digestible carbohydrates [55]. They have been positively associated with body weight reduction and insulin sensitivity, which are considered as one of the functional mechanisms of probiotics [56, 57]. In addition, SCFAs are also ligands and activators of G protein-coupled receptors (GPRs), including GPR41 and GPR43, renamed as FFAR3 and FFAR2, respectively [58]. The activation of these

receptors by butyrate and propionate leads to the enhanced secretion of satiety hormones in the intestine. Specifically, it has been reported that the *ffa2*-deficient mice displayed the lower glucagon-like peptide-1 (GLP-1) secretion, while the *ffa3*-deficient mice revealed a reduced peptide YY (PYY) expression [59, 60]. Consequently, the overexpressed receptors activated by SCFAs result in the decreased energy consumption and alleviates obesity [61-63].

Clostridium cochlearium

The potential probiotic of interest in this study was *Clostridium cochlearium* (*C. cochlearium*). It has been found in mammalian gut microflora, such as the rat, mice, and humans, suggesting its common and nonpathogenic nature [64, 65]. *C. cochlearium* is a Gram-positive anaerobic bacteria that belongs to the genus of *Clostridium*, which has a wide range of functions [66]. Some species in the genus of *Clostridium* have been identified as the pathogens, such as *C. botulinum*, *C. perfringens*, and *C. difficile* [66-68]. However, certain species of *Clostridium* have been shown to possess probiotic effects [67]. For example, *Clostridium butyricum*, named after its main product, butyric acid [69], has been suggested as a probiotic to prevent and treat obesity and other metabolic syndromes [70, 71]. Currently, there are limited references related to the health effect of *C. cochlearium*; however, it has properties similar to that of *C. butyricum*, such as converting carbohydrates into butyrate and other SCFAs [72, 73]. Studies have shown that dietary supplementations of butyrate or butyrate producers, such as *Eubacterium hallii*, reduced insulin resistance in *db/db* mice [74, 75], suggesting a beneficial role of butyrate in improving obesity-related complications. Thus, *C. cochlearium* could be a potential novel probiotic against obesity and its related complications.

Specific aims

The overall goal of this investigation was to determine the potential probiotic effect of *Clostridium cochlearium* supplementation on high-fat diet-induced obesity in C57BL/6mice and to further determine the underlying mechanism in relation to SCFAs and gut microbiota modification. We hypothesized that dietary supplementation of *C. cochlearium* could change gut microbiota and increase butyrate production in the gut, consequently reducing body weight gain in high fat-induced obese mice. To test our hypothesis, we proposed three specific aims.

Aim 1 was to determine the effect of *C. cochlearium* supplementation on high-fat diet-induced obesity and its associated complications using a mouse model.

Aim 2 was to determine the effect of dietary *C. cochlearium* treatment on gut microbiota via 16S rRNA gene sequencing. Continuous supplementation of *C. cochlearium* was expected to significantly alter the gut microbiota.

Aim 3 was to determine whether the probiotic effect of dietary *C. cochlearium* treatment is mediated through modification of gut microbiota and SCFAs production. Functional gene analysis was used to determine the potentially related gut microbial enzymes and their corresponding metabolic pathways. Additional gene expression was analyzed to confirm the potential interaction between host and gut microbiome based on the predicted potential pathways.

CHAPTER 2. DETERMINE THE EFFECT OF *C. COCHLEARIUM* SUPPLEMENTATION ON A DIO MOUSE MODEL

In order to mimic human obesity development, a diet induce-obesity (DIO) animal model would be suitable for the evaluation of the phenotypical and genetic effects of a high-fat Western diet. For this purpose, the C57BL/6 mouse model was chosen for this study. Currently, there are limited animal studies related to *C. cochlearium*, so no *in vivo* reports were available on its health effect. As a butyrate producer, it was hypothesized that *C. cochlearium* is able to modify glucose homeostasis and further prevent obesity development. Our objective was to investigate whether dietary *C. cochlearium* can reduce body weight gain in DIO mice treated with a high-fat diet. We conducted a 16-week dietary intervention. Mouse body weight was recorded weekly in order to monitor the weight change. In addition, the body composition of each mouse was evaluated using an MRI analyzer at the end of dietary treatment to determine the supplemental effects on fat mass and lean mass. Glucose homeostasis analysis, including periodic fasting blood glucose test, oral glucose tolerance test (OGTT), and insulin sensitivity, was performed. Energy balance of each mouse was evaluated at the end of treatment, which included food intake, fecal energy content, and energy expenditure.

Methods

Bacterial preparation

C. cochlearium strain (ATCC 17787) was purchased from ATCC (Manassas, VA). They were cultured using anaerobic PYG media and conditions according to the previously recommended method [76]. The cultured bacteria were collected and centrifuged to yield a bacterial pellet at the end of the growth phase. The pellet was then washed with sterile phosphate-buffered saline and integrated with sterile 25% glycerol in PYG media to reach the final

concentration of 10^{10} CFU/mL. The serial dilution and plating methods were utilized to check the viability to ensure the desired concentration for all further experiments. The bacterial glycerol stock was flash-frozen in liquid nitrogen and stored at -20°C . The preparation was used within one week. During the experiment, bacterial samples were prepared daily at 30 min – 1 hour before oral gavage using thawed *C. cochlearium* glycerol stock. It was then centrifuged and washed with sterile phosphate-buffered saline to remove any excess storage medium. The final *C. cochlearium* culture was resuspended in sterile water and ready for oral gavage.

Experimental animals

The experiment was conducted with the approval of the Institutional Animal Care and Use Committee (IACUC) of Wayne State University. Thirty-six 6–8-week-old male C57BL/6 mice were purchased from Charles River Laboratories (Wilmington, MA), and housed in the Biological Science Building under 12-hour day/night cycles, constant room temperature ($24^{\circ}\text{C} \pm 1^{\circ}\text{C}$), and controlled moisture level ($40\% \pm 10\%$). Food and water were given ad libitum. To prevent the possible intake of bedding material, sani-chip bedding was prepared for each cage. Two kinds of rodent diets were provided, the high-fat diet (D12492M) and the low-fat diet (normal diet, D12450J), which were stored at 4°C until use. Both were purchased from Research Diets Inc. (New Brunswick, NJ). The high-fat diet contained 5.24 kcal per gram with 60% of calories from fat and 20% of calories from carbohydrates, while the low-fat diet consisted of 3.85 kcal per gram with 10% from fat and 70% from carbohydrates. The nutrition composition of these purified rodent diets is disclosed in Table 1. After 7-day acclimatization with the low-fat diet, mice were randomized into three groups ($n = 12$ per group, six mice per cage): the high-fat diet (HF) control group, the low-fat diet control (LF) group, and the *C. cochlearium* supplemented high-fat diet (CC) group. The HF control and LF control groups were gavaged with 200 μL of sterile water, while

the experimental group (CC) was treated with 200 μ L of *C. cochlearium* culture containing approximately 10^{10} CFU/mL along with the high-fat diet. The experimental duration was set to be 16 weeks. Food intake and body weight were monitored weekly.

Fecal energy analysis

At week 12, fecal pellets were collected and pooled from each cage within a 24-hour period while food and water were still provided to all the mice. All pellets were then air-dried and stored at -20°C for further analysis. Fecal energy was measured using a Bomb Calorimeter (Parr, Moline, IL). Duplicated fecal pellets (0.5 g per cage) per group were weighed and combusted in the calorimeter to yield appropriate energy output. The actual quantity of burned fecal content was used to calculate the fecal energy (kcal/g), where post-test non-combustible residue weight was subtracted from pre-test fecal weight. Additionally, feed efficiency was calculated using the following formula: Feed efficiency = total mouse body weight gain / total energy intake \times 100%.

Glucose homeostasis

Fasting blood glucose was evaluated every four weeks, during which each mouse's tail vein blood drawn was tested with an Accu-chek glucometer (Roche, Indianapolis, IN) post-8-hour fasting with only water given. At week 15, an oral glucose tolerance test (OGTT) was performed for each mouse. After 8-hour food deprivation with only water given, all mice were given a glucose solution (10% w/v in sterile water) at the dosage of 1 g per kg body weight via oral gavage. At the time point of 0, 15, 30, 60, and 120 min, blood glucose was measured with an Accu-check glucometer via tail vein sampling. Incremental areas under the curve (AUC) of blood glucose levels were calculated using the standard trapezoid method [77].

Serum fasting insulin was evaluated followed the manufacturer's instruction using the ultra-sensitive mouse insulin ELISA kit (Crystal Chem, Doners Grove, IL). The optical density

(OD) values were tested using a microplate reader with 450 nm and 630 nm filters. The standard curve of insulin was produced to compute the serum insulin levels. Samples were measured in duplicates and the average of these 2 duplicates was calculated for each sample. The average absorbance value of each sample and the standard curve were used to interpolate the sample's OD values. Homeostatic model assessment of insulin resistance (HOMA-IR) was computed as follows: $\text{fasting insulin (mU/L)} \times \text{fasting glucose level (mg/dL)} / 405$ [78].

Metabolic study and body composition analysis (BCA)

At week 15, each mouse from the HF group and the CC group was transferred to Wayne State University iBio facility and caged for five days (with 2-day acclimatization) into TSE PhenoMaster metabolic chamber system (TSE Systems, Chesterfield, MO) in order to measure each mouse's energy expenditure and activity level. The housing environment for the mice was maintained the same as the previous group housing condition with the same light (day) /dark (night) cycle. Food consumption and weight changes of each mouse were measured and recorded along with respiratory parameters, including heat emission, respiratory exchange ratio (RER) via CO₂ production/O₂ consumption. In addition, each mouse's activity levels were also measured using horizontal and vertical infrared motion sensors spread out around the housing cage. Movement units were then converted into the distance in centimeters or meters for analysis. BMR was calculated based on the mean heat emission from the 10 lowest successive time points (kcal per 24 hours) and then divided by each mouse's body weight.

After metabolic analysis, body composition was measured using the EchoMRI-100 analyzer (EchoMRI, Houston, TX) at the same building. Oil standard was used as the calibrator to accurately measure body density differences when placed in the MRI scanner. Each mouse was weighed prior to scanning, and duplicated measurements were performed and resulted in fat and

lean mass, which would be further calculated into percentages. Free water such as blood and urine were subtracted from the total weight of the animal for accurate fat/lean ratio analysis. The fat percentage, lean mass percentage, and fat/lean ratio were calculated using the following formulas: fat percentage = fat mass/weight \times 100%. Lean mass percentage = lean mass/weight \times 100%. Fat/lean ratio = fat mass/lean mass.

Euthanasia and tissue collection

Upon termination, all mice were euthanatized by CO₂ exposure with subsequent cervical dislocation. The heart puncture method was used for blood collection, and approximately 1 to 1.5 mL of blood samples were able to be collected and placed into sterile Eppendorf® microtubes. The samples were then left undisturbed at room temperature for 30 minutes after the collection. In order to remove the clot, the blood samples were centrifuged (1000 g, 10 minutes, 4 °C), and the supernatant was aliquoted into microtubes. All serum samples were then aliquoted and flash-frozen in liquid. Tissues (liver, kidney, and fat) from each mouse were collected, weighed, and quenched immediately using liquid nitrogen. Intestinal contents from the cecum and large intestine (absent of solid fecal droplet) were scrapped out and placed in microtubes, which were immediately flash-frozen in liquid nitrogen. All samples were stored at -80 °C until analysis.

Statistical analysis

Data were analyzed and presented as means \pm SEM. Statistical analyses of the three groups of data were performed using one-way or two-way analysis of variance (ANOVA) followed by a post-hoc t-test with Turkey correction by GraphPad Prism (V 7.0, La Jolla, CA). The metabolic data between the HF and CC groups were performed using the Student t-test with GraphPad Prism. All the results were considered statistically significant at $P < 0.05$.

Results

The body weight trends between the LF, HF, and CC groups during the 16-week intervention are presented in **Figure 1**. The HF group gained body weight at the highest rate, followed by the CC and LF control groups. At the third week of dietary intervention, mice in the CC group started to show significantly less body weight than the HF group. The difference remained significant until the end of the dietary intervention. After 16 weeks of the high-fat diet treatment, the HF mice gained 101.4% from original body weight, while the high-fat diet supplemented with *C. cochlearium* was able to reduce body weight gain to 85.6% (**Table 2**). The average body weight of the CC group was 7.6 g less than that of the HF group, which accounted for a 14.8% reduction in the CC mice when compared to the HF group ($P < 0.0001$). The CC group had a significantly reduced percentage body weight gain of 15.8% compared to the HF group ($P < 0.0001$).

The body composition of each mouse in the LF, HF, and CC groups was evaluated at week 16 of the intervention as shown in **Table 2**. The HF group had the highest fat mass and fat percentage across the three groups, which were significantly higher than that of the CC group ($P < 0.0001$, $P < 0.05$, respectively). Specifically, the fat mass in the CC mice was decreased by an average of 20.8% compared to the HF mice. The LF group showed the lowest fat mass and fat percentage among the three groups. The average lean mass of the CC mice was lower than that of the HF mice ($P = 0.06$). However, there was no significant difference in the lean mass percentage between the two groups ($P > 0.05$). In addition, the CC group had a significantly lower fat/lean ratio than the HF group did ($P < 0.01$).

Fasting blood glucose levels were performed every 4 weeks. **Figure 2** shows that the serum fasting glucose levels of the HF group were higher than for the other two groups after the eighth

week. There was no significant difference in fasting blood glucose between the CC and LF groups throughout the dietary intervention. At the end of the intervention, the CC group maintained an average fasting blood glucose level of 175.2 ± 10.3 mg/dL (**Table 3**), which was reduced by 21.7% when compared to the HF group.

Additionally, the oral glucose tolerance test was also performed for all three groups at the time points of 0, 15, 30, 60, and 120 minutes following ingestion (**Figure 3**). The HF group showed significantly higher blood glucose levels than the other two groups at all time points. The blood glucose response in OGTT also showed a significant difference by *C. cochlearium* treatment as compared to the high-fat diet-only treatment. *C. cochlearium* treatment improved the glucose tolerance and subsequently returned the blood glucose back to a normal level at the end of OGTT. The area under the curve (AUC) was calculated based on the results of OGTT glucose levels, as shown in **Figure 4**. The HF group showed a significantly elevated AUC level compared to the LF ($P < 0.0001$) and CC groups ($P < 0.0001$), while the AUC level of the CC group was also significantly higher than that of the LF group ($P < 0.0001$). Specifically, the AUC level of the CC group was 39.8% lower than that of the HF mice.

The fasting insulin and glucose levels were measured at the end of the intervention in order to compute the HOMA-IR (**Table 3**). The average insulin level of the CC group was significantly lower than that of the HF group ($P < 0.01$), which was reduced by 36.9% in the CC group when compared to that of the HF group. The HOMA-IR calculation has confirmed that the HF group had a significantly elevated level compared to the CC group ($P < 0.01$), which showed a 47.2% reduction in the CC group compared to the HF group ($P < 0.01$).

The food intake was monitored every week, and the average energy consumption was calculated (**Table 4**). Due to the lower energy in the normal diet, lower grams of food consumption

were observed in the HF and CC mice compared to the LF group. After calculating diets into calories, similar daily food intake was observed among the 3 groups. The HF group showed the highest fecal energy output at 1.3 kcal/day/mouse when compared to the LF and CC groups ($P < 0.0001$, $P < 0.0001$, respectively). Subsequently, the feed efficiency analysis using daily total caloric intake per weight gain generated a significantly higher ratio in the HF group compared to the CC group ($P < 0.01$). Interestingly, the calorie absorption was significantly higher in the CC group compared to the HF group ($P < 0.001$).

The respiratory exchange ratio (RER) was calculated based on the quantity of carbon dioxide generated in metabolism and oxygen utilized. The RER of the HF group was lower than that of the CC group ($P < 0.05$) (**Table 4**). Similarly, the HF group had a lower basal metabolic rate (BMR) than the CC group did ($P < 0.05$). The daily physical activity level was measured in average distance traveled (meters/day/mouse), which indicated that mice in the CC group were more active than the HF group ($P < 0.05$).

Discussion

The results of this study confirmed the effects of a high-fat diet on C57BL/6 mice as expected based on previous literature reports, including body weight gain, insulin resistance, hyperglycemia, and increased fat mass [79, 80]. A study by Siersbæk et al. indicated that the body weight gain of C57BL/6J mice increased approximately by 80% at week 10 with high-fat diet treatment, which is similar to our results [80]. Our HF group had body weight gain increase by 73.2% at week 10 and 82% at week 11. The dietary supplementation of *C. cochlearium* also supported our hypothesis that *C. cochlearium* can reduce high-fat diet-induced obesity and its associated complications, such as increased body weight gain, fat mass, fat percentage, and fat/lean ratio. A significant decrease in fat mass in the CC group was observed, which has been correlated

with the lower risks of several chronic diseases, such as diabetes, cardiovascular disease, and cancer [81]. In our investigation, since there is no difference in lean mass percentage, the major body weight difference between the HF mice and CC mice came from the significantly shifted fat mass/fat percentage. The reduced fat mass by *C. cochlearium* supplementation would be associated with SCFAs. SCFAs-activated *ffar2* genes from fat tissue suppress insulin metabolism in adipose cells and subsequently reduce fat storage and promote glucose signaling in other tissue [63]. As a butyrate producer, the *C. cochlearium* supplemented group promotes SCFAs production, which could lead to less fat mass compared to the HF group.

Glucose homeostasis was another point of interest when examining the efficacy of *C. cochlearium* supplementation. The fasting glucose during the whole period of intervention has clearly indicated the significant difference between the HF group and the CC group as described above, suggesting the administration of *C. cochlearium* significantly reduced the fasting blood glucose level and improved the glucose tolerance and insulin sensitivity. Although the fasting glucose level was similar in the LF and CC groups, both AUC and HOMA-IR were significantly higher in the CC group compared to the LF group. This could be due to the administration of *C. cochlearium*, which partially reduced the onset of insulin resistance caused by a high-fat diet but might not be enough to reverse the insulin resistance to the level observed in the low-fat-fed mice. Although no previous study has investigated *C. cochlearium* in glucose homeostasis, these results are consistent with other similar property probiotics. *Clostridium butyricum* (*C. butyricum*), a butyrate producer as well, has been shown to improve fasting glucose and insulin sensitivity in high-fat diet-induced diabetic mice by gut microbiome modulation with elevated butyrate-producing bacteria [71]. Thus, our *C. cochlearium* supplementation could have a similar mechanism through the alteration of the gut microbiome. Exploring the microbiome profile is

needed to clarify the potential mechanism through the shifted gut composition. In conclusion, *C. cochlearium* supplementation had the ability to reduce fasting blood glucose and improve insulin sensitivity.

Food intake, fecal energy, and activity level were measured in order to analyze the energy balance. There was no difference in energy intake among the tested groups. The HF mice had a higher fecal energy content than the CC group did. Nevertheless, the reduced body weight gain and fat mass in the CC group should be the result of increased energy expenditure. The elevated feed efficiency in the HF group suggested that the CC mice reduced energy storage, which resulted in a lower fat mass and fat percentage, as hypothesized. Moreover, mice's RER (VCO_2/VO_2) through indirect calorimetry analysis revealed a significantly higher ratio in the CC group than that of the HF group, suggesting that mice in the CC group utilized relatively less fat and more carbohydrates as energy fuel than mice in the HF group did [82]. RER values indicated that both the HF and CC groups showed mixed respiratory substrates; however, it might be associated with potential elevation of the SCFAs production pathway as mentioned above [63]. This theory is not yet well understood as our hypothesis of weight reduction through fat mass decrease could be due to increased fatty acid oxidation, which would have given a lower RER in the CC treatment group. Therefore, further investigation into the *in vivo* SCFAs production along with organ-specific metabolism, such as liver- and adipose-specific SCFAs receptors, could be helpful to elucidate the mechanism. Approximately 10.7% increase in BMR was observed from the CC group when compared to the HF group, suggesting that the CC mice utilized more energy for basal energy needs. This is consistent with a previous study that showed BMR was lower in obese people than the normal weight counterparts [83]. Furthermore, the physical activity level measured by the traveled distance in the metabolic chamber was 98% higher in the CC group compared to those in

the HF group. Both physical activity and BMR level have been involved with fat oxidation, which could explain the reduced body weight gain and lowered fat mass observed in the CC group [84, 85]. The elevated energy expenditure could also be associated with the gut microbiome. Although mechanisms between the increased energy expenditure and influences from the gut profile shift are not yet clear, SCFAs produced by gut microbiota have been suggested to increase energy expenditure through fat oxidation, which promotes the host activity level [86]. Thus, the production of SCFAs from bacteria might explain the increased energy expenditure, especially the elevated physical activity of the host. Therefore, the next step was to analyze the gut microbiome differences between the HF and CC groups.

CHAPTER 3. DETERMINE THE EFFECT OF DIETARY *C. COCHLEARIUM* TREATMENT ON GUT MICROBIOME PROFILE VIA 16S rRNA GENE SEQUENCING

Over the last decade, biologists have raised the importance of the gut microbiome inhabited by thousands of bacterial species in diverse communities unique to each body site [87]. It is becoming evident that the gut microbiome plays an important role in human health and disease [88]. In order to understand the gut microbiome, 16S rRNA gene sequencing has become the approach to explore the gut microbiome by identification, classification, and quantitation of microorganisms. The 16S rRNA gene includes both variable regions used for microbiota identification and conserved regions used for designing universal PCR primers [89]. The V3 and V4 regions are hypervariable, commonly used in 16S sequencing [90]. In our investigation, V4 regions of the encoding gene were amplified and sequenced. It was hypothesized that the gut microbiome in the CC group would be modulated by supplemented *C. cochlearium* compared to the HF group. The shifted profile was analyzed to explore how *C. cochlearium* supplementation contributes to gut microbiome communities.

Methods

16S rRNA-amplicon sequencing of gut microbiota

The intestinal content collected was utilized for bacterial community composition analysis. Samples were sent to, as well as extracted and analyzed by, the University of Michigan Microbial Systems Molecular Biology Laboratory (MSMBL), Ann Arbor, Michigan. DNA extraction was processed by the Qiagen MagAttract PowerMicrobiome kit (Qiagen, CA, USA) and following the manufacture's protocol. The Quant-iT PicoGreen dsDNA Assay kit was used to quantify the DNA samples. The V4 hypervariable region of the 16S rRNA-encoding gene was amplified, normalized,

and sequenced by MiSeq Reagent Kit v2 (500 cycles) on the Illumina MiSeq platform (San Diego, CA, USA) [91].

Sequencing data were analyzed using QIIME 2 software (2019.12) [92]. After demultiplexing and quality filtering using the q2-demux plugin, denoising was followed via q2-dada2 [93]. The denoised sequences were then clustered into operational taxonomical units (OTUs), which involved using 97% sequence similarity against a reference Greengenes OTU database (Release 13.8) for taxonomic classification [94-96]. Alpha-diversity was measured, including Shannon diversity index, Pielou's evenness, and Faith's phylogenetic diversity. The beta-diversity metrics were estimated using the Principal Coordinate Analysis (PCoA) based on UniFrac (unweighted and weighted) distance, Jaccard distance, and Bray-Curtis dissimilarity. Both alpha and beta diversity analyses were computed using q2-diversity. Kruskal-Wallis test and Permutational multivariate analysis of variance (PERMANOVA) were further implemented using q2-diversity-alpha-group-significance/beta-group-significance to evaluate the group difference for alpha diversity box plots and the group separation for PCoA, respectively.

The linear discriminant analysis (LDA) effect size (LEfSe) was analyzed to explore high-dimensional biomarker taxa with significantly varied relative abundance between two groups [97]. The Kruskal-Wallis rank sum test among classes was used to detect the differences of species abundance with the alpha level of 0.05. The threshold of 2.0 was used on the logarithmic LDA score for discriminative features [97, 98].

Statistical analysis

The relative abundance of the gut microbiome at the phylum level was presented as means \pm SEM. Statistical analyses between the HF and CC groups were performed using Student's t-test by GraphPad Prism (V 7.0). Results were considered statistically significant at $P < 0.05$.

Results

In total, 5,390,372 sequencing reads were obtained from 22 mouse intestinal content samples of the HF group ($n = 12$) and the CC group ($n = 10$), with an average of 449,198 reads per sample. After the quality filtering and denoising, 20 sample taxonomies were assigned by the Greengenes 13_8 97% OTUs taxonomy classifier. The relative abundance was converted by Qiime 2 2019.12, as shown in **Figure 5**. Firmicutes, Proteobacteria, and Bacteroidetes were predominant of the total community at the phylum level and accounted for 95.46% and 95.18% of the HF and CC groups, respectively. Specifically, Bacteroidetes and Proteobacteria were elevated in the CC group as compared to the HF group ($P = 0.068$, $P < 0.05$, respectively) (**Table 6**). Firmicutes showed significantly lower abundance in the CC mice than in HF mice ($P < 0.05$). One of the minor phylum groups, Tenericutes, showed a significant difference between the HF and CC groups ($P < 0.001$). The ratio of Firmicutes to Bacteroidetes (F/B) was then calculated, which yielded a significantly lower ratio for the CC group than that of the HF group ($P < 0.05$).

The alpha-analysis was used to measure the microbiome diversity, including non-phylogenetic metric and phylogenetic metric [99]. In this study, Pielou's evenness and Shannon diversity index were performed as non-phylogenetic metrics, while Faith's phylogenetic diversity was used as a phylogenetic metric. The gut bacteria in the CC group showed a significantly higher level in both Pielou's evenness ($P < 0.001$, **Figure 6**) and Shannon diversity index ($P < 0.001$, **Figure 7**) by the Kruskal-Wallis test. There is no significant difference in Faith's phylogenetic diversity (**Figure 8**) among the HF group and the CC group, even though the gut microbiota of the CC mice showed an elevated level of diversity compared to that of the HF mice.

The beta-analysis was performed to estimate the difference between two composition vectors, which measured the amount of species shift between regions [100]. Unweighted UniFrac,

weighted UniFrac, Bray-Curtis, and Jaccard distance PCoA plots are depicted in **Figures 9-12**. The UniFrac-based PCoA indicated significant separation between the HF and CC groups for both unweighted ($P = 0.001$) and weighted ($P = 0.001$) plots as shown in **Figure 9** and **Figure 10**. The first three components of unweighted UniFrac explained 41.71% of the total variance (17.46%, 14.82%, and 9.43% for PC1, PC2, and PC3, respectively), while the first three components of weighted UniFrac covered 74.39% of the total variance (43.96%, 16.73% and 13.70% for PC1, PC2, and PC3, respectively). The Bray-Curtis PCoA has also confirmed the significant separation between the HF and CC groups based on the microbial abundances (**Figure 11**). The Jaccard PCoA indicates that the CC group was significantly distinct from the HF group based on the presence of species (**Figure 12**). All four beta-analysis plots were further analyzed by PERMANOVA, which all showed significant separation with $P = 0.001$.

LEfSe was performed with a list of 69 OTUs that summarized to genus. The LDA score, which was transformed to a logarithmic plot, was performed to estimate the influence of the differential abundance between the HF and CC groups depicted in **Figure 13**. All the species shown in **Figure 13** were significantly contributed to their microbial profile filtering by the Kruskal—Wallis test, which clarified the differences between the HF and CC groups. The higher the LDA value of a specific species means the more important the species to its microbial group (HF or CC group). The threshold was set as 2, which means that the LDA score plot only indicated the absolute score over 2. The cladogram shown in **Figure 14** was another output of LEfSe analysis, which added the taxonomy classification of those contributing bacteria. There are circles in **Figure 14** from the inside to the outside, which represent the bacteria classification level from the phylum to the genus. The larger the circle size indicates the higher relative abundance of the bacteria. There are three colors of circles shown in the cladogram. The bacteria without any significant differences

between the HF and CC groups are yellow. The significantly different microbiota between the HF and CC groups are green and red, respectively. In this case, the red circles of bacteria significantly higher abundance in the CC group, while the green nodes played a significant role in the HF group. Combining with both LDA score plots and the cladogram, several bacteria were found the differential abundance between the HF and CC groups. In the CC group, both the family of *Ruminococcaceae* and its genus of *Ruminococcus*, *Oscillospira*, and *Clostridium* significantly supported the CC group. The family of *Lachnospiraceae* with its genus of *Dorea* and *Ruminococcus*, the family of *Desulfovibrionaceae* with its genus of *Bilophila*, the family of *Xanthomonadaceae* with its genus of *Stenotrophomonas*, the family of *Moraxellaceae* and its genus of *Acinetobacter*, the family of *Mogibacteriaceae*, the family of *Christensenellaceae*, the family of *Rikenellaceae* and the family of *S24_7* played an important role in the CC group when compared to the HF group. Although there is no *C. cochlearium* specifically shown in the LEfSe results, its genus of *Clostridium* has shown a significant contribution to an altered microbiome in the CC mice. In the HF group, the family of *Lactobacillaceae* and its genus of *Lactobacillus*, the family of *Streptococcaceae*, and its genus of *Streptococcus* and *Lactococcus*, the family of *Enterobacteriaceae* and its genus of *Escherichia*, and the family of *Peptostreptococcaceae* strongly contributed to the microbiota profile of the HF group.

Discussion

Probiotics have the ability to attain their anti-obesity beneficial effects by modifying the gut microbiome profile and consequently enhancing intestinal barrier function or boosting the host's immunity [101]. In this study, the alteration of *C. cochlearium* supplementation was evaluated using alpha- and beta-diversity analysis. The detailed modulated microbiota, especially

at the phylum level, family level, and genus level, were detected and analyzed to display the contribution of gut microbiota to the anti-obesity effect by the administration of *C. cochlearium*.

The alpha-diversity analysis was used to measure the species diversity of each sample at the local region and compare the difference of richness between groups. Among the non-phylogenetic metrics of alpha-diversity indices, Pielou's evenness is the estimator for the evenness of species abundance, while the Shannon diversity index was estimated based on both richness of species numbers and evenness of species abundance [99, 102]. For the phylogenetic metrics, Faith's phylogenetic diversity was performed in this study to estimate based on both abundance information and phylogenetic information [99]. In this intervention, significant elevation of Pielou's evenness and Shannon diversity index in the CC group was observed when compared to the HF group, suggesting that the administration of *C. cochlearium* significantly increased the evenness and richness of gut microbiota. In Faith's phylogenetic diversity box plot, the increase of diversity in the CC group was also observed, but there was no significant change between the HF and CC groups. Overall, the increased diversity of gut bacteria, which is associated with anti-obesity, was shown in the CC group compared to the HF group [103-105]. The high microbial diversity has been correlated with less fat mass and insulin resistance [105]. It is consistent with the animal study results that the fat mass and HOMA-IR were significantly lower in the CC group than in the HF group. Moreover, reduced microbial diversity has been observed in seniors with intestinal inflammation and patients with ulcerative colitis, inflammatory bowel disorder, and dyslipidemia [105-108].

The beta-diversity analysis was performed to evaluate the change in species diversity between the HF and CC groups. In this investigation, both unweighted and weighted UniFrac distance, Bray-Curtis dissimilarity, and Jaccard distance were measured. The UniFrac distance

was analyzed based on the sequence distances, also known as the phylogenetic tree [109]. Specifically, the unweighted UniFrac purely contains the sequence information, while the weighted UniFrac incorporated both abundance and sequence information [109]. Bray-Curtis dissimilarity was used to evaluate the differential abundance of gut microbiota between the HF and CC groups, while the Jaccard distance assessed the differential composition of gut bacteria among the two groups [109, 110]. Jaccard distance was analyzed based on the existence or absence of a species without the abundance data [110]. All four measurements comprehensively analyzed the differences in gut microbiome composition between the HF and CC groups. All of the measurements' PCoA plots depicted the strong separation between the HF and CC groups and were further analyzed by the PERMANOVA, which revealed the significant differences in gut microbial composition between the two groups. This suggested that the *C. cochlearium* supplementation significantly modulated the gut microbiome profile with regards to the abundance, presence, and phylogenetic information of bacteria.

The gut microbiota is mainly comprised of two predominant phyla, Firmicutes and Bacteroidetes, and other subdominant phyla, including Proteobacteria, Actinobacteria, and Verrucomicrobia [111]. Based on our findings, Firmicutes and Bacteroidetes were still the dominant phyla in both the HF and CC groups. Firmicutes were observed with a significant reduction in the CC group, which was approximately 6.8% lower than the HF group. The elevation trend of Bacteroidetes in the CC group was also displayed when compared to the HF group with the $P = 0.068$. The F/B ratio has been frequently mentioned in the literature related to obesity [112, 113]. It has been widely reported that the finding of increased Firmicutes and decreased Bacteroidetes were discovered in high-fat DIO mice and obese *ob/ob* mice compared to their lean controls [114, 115]. According to the literature, Firmicutes have been found to be more effective

in absorbing energy than Bacteroidetes and subsequently promoting weight gain [35, 111, 116]. Consequently, a high F/B ratio has been frequently linked with higher body weight or the body mass index (BMI) as a hallmark of obesity [36, 112, 113]. Moreover, the physical activity level has also been inversely correlated with the F/B ratio in animals and humans [111]. The outcome of our animal studies confirmed a similar phenotype as previous F/B ratio-related literature, in which the *C. cochlearium* treatment group showed reduced body weight gain and higher activity level compared to the HF group. Thus, this suggested that reducing the F/B ratio could be one of the reasons that the administration of *C. cochlearium* had anti-obesity activity.

Furthermore, the phylum of Proteobacteria was shown to be positively associated with gut dysbiosis and metabolic diseases, and it was suggested as a “microbial signature” [117]. However, an elevated abundance of Proteobacteria was also observed in a dietary supplementation of a whole-grain oats animal study conducted by Zhou et al. The study suggested that a higher abundance of Proteobacteria has been associated with enhanced insulin sensitivity in C57BL/6J mice [77]. These inconsistent findings were likely due to the use of diverse animal models, insufficient amounts of subjects, or nonuniform experimental protocols [118-120]. Further investigation and comparison with other literature on the specific genus or species level to determine whether Proteobacteria could influence the overall profile or F/B ratio would be helpful to gain further perspectives.

The output of LEfSe analysis displayed the significantly differentially abundant bacteria for the HF group and the CC group. The family of *Ruminococcaceae* and its genus of *Ruminococcus*, *Oscillospira*, and *Clostridium* has been detected as a significant contribution to the CC group. The family of *Ruminococcaceae* bacteria has been shown to be butyrate, lactate, and acetate producers [121]. The abundance of the *Ruminococcaceae* family has been associated with

the anti-obesity effect, with the potential of reducing the risks for obesity and cardiometabolic disease [122, 123]. Moreover, the family of *Ruminococcaceae* has been negatively associated with ulcerative colitis, one of the inflammatory bowel diseases [107]. Therefore, *C. cochlearium* supplementation could beneficially influence gut microbiota in ameliorating adverse digestive tract diseases.

Moreover, the family of *Lachnospiraceae*, which can ferment carbohydrates into SCFAs as well, has been detected in increased abundance in the CC group when compared to the HF group [124]. The decreased abundance of the family of *Lachnospiraceae* bacteria was noticed in the obese participants in another clinical trial [122]. Another animal study has proved that the family of *Lachnospiraceae* diminished body weight gain, body fat, and microbiome dysbiosis, and improved glucose homeostasis in *Nlrp12*^{-/-} mice [124]. The abundance of *Lachnospiraceae* bacteria was inversely associated with colorectal cancer, ulcerative colitis, and cirrhosis dysbiosis as well [107, 125, 126]. Interestingly, although the *Lachnospiraceae* family is not associated with obesity, the genus of *Dorea* and *Ruminococcus* under the family of *Lachnospiraceae*, which were also shown the contribution to the change in the CC group, has been associated with obesity and inflammatory bowel disease [127-129]. It might be because the *C. cochlearium* supplementation attenuated the high-fat-induced obesity but cannot comprehensively reverse the consequences of obesity.

Other significant differential abundant taxa in the CC group, the families of *Christensenellaceae*, *Mogibacteriaceae*, *Rikenellaceae*, and *S24_7*, have been associated with anti-obesity effect and increased bowel movement [127, 130]. Among these, the family of *Christensenellaceae* has been described as SCFAs producer [131]. In a recent twin cohort study, the family of *Christensenellaceae* was found as the most heritable taxon, and the abundance of the

Christensenellace family was negatively associated with BMI [132]. Moreover, the family of *Christensenellace* has been linked to longevity in several cohort studies across diverse geographic areas [133].

Most of the gut microbiota mentioned above with increased abundance in the CC group are SCFAs producers. Some taxa with significantly higher abundance in the CC group cannot directly produce SCFAs, but have a positive correlation with the intestinal concentrations of SCFAs (acetate and propionate), including the genus of *Stenotrophomonas* and the family of *Desulfovibrionaceae* [134, 135]. Therefore, the administration of *C. cochlearium* potentially modulated the gut microbiome composition also by influencing the SCFAs-producing bacteria abundance. Most of the SCFAs-producing bacteria, especially for the butyrate-producing bacteria, are beneficial and play an important role in the anti-inflammatory effect [136].

The increased abundance of class Bacilli and its families *Streptococcaceae* and *Lactobacillaceae* were correlated with obesity [122]. This is consistent with our findings from the HF group. It is interesting to observe that the genus of *Lactobacillus* under the family of *Lactobacillaceae* had a significant contribution to the HF group. It has been widely reported that *Lactobacillus sp.* are beneficial, and can be used and added as probiotics in food, such as *Lactobacillus acidophilus* and *Lactobacillus rhamnosus* [137, 138]. However, some species of *Lactobacillus*, such as *Lactobacillus acidophilus*, *Lactobacillus fermentum*, *Lactobacillus ingluviei*, and *Lactobacillus reuteri*, have been associated with weight gain in animals [139-142]. Surprisingly, the abundance of the *Lactococcus* genus from the family *Streptococcaceae* was higher in the HF group compared to the CC group. *Lactococcus* genus is famous for *Lactococcus lactis*, a probiotic that was positively correlated with insulin sensitivity [54, 143]. However, not all the species in the genus of *Lactococcus* are probiotics. *Lactococcus lactis cremoris*, *L. lactis*

subspecies, has been reported as a rare pathogen that can cause human infections [144]. In our investigation, we cannot identify the specific species of the *Lactococcus* genus contributing to the HF group. Thus, the influence of the increasing abundance of the *Lactococcus* genus is uncertain.

The LEfSe output has confirmed that the phylum level differentiation between the HF and CC groups as previously analyzed relative abundance results. Moreover, the most significant taxonomy changes in the CC group were SCFAs-producing or related bacteria and associated with the anti-obesity effect. On the contrary, majority of the highly abundant taxa in the HF group were linked to pro-obesity. Overall, it can be concluded that the administration of *C. cochlearium* had an effect against obesity through the alteration of gut microbiome composition by a potential SCFAs metabolic pathway.

Although the genus of *Clostridium* under different families showed a significant difference between the HF group and the CC group, there is no *C. cochlearium* detected in the OTU table from the sequencing analysis results provided. One of the potential reasons could be identified as unclassified species in the OTU table, which may contain *C. cochlearium*, and was reflected as a significant increase of *Clostridium* genus in the CC group. In addition, the reference database we used in this study is the Greengenes database, which is based on the information from other taxonomy sources, mainly from NCBI [145]. Likewise, the most updated Greengenes database version was released in 2013, which means it has not been updated for almost 8 years [145]. Secondly, there could be a difficulty in the extraction of genetic materials of *C. cochlearium* from the low quantity of intestinal content, likely leading to non-detectable quantity. It is also possible that the supplemented *C. cochlearium* could have started sporulation, which may affect extraction and detection [146, 147]. We also suspected the possibility of microbial profile change due to the *C. cochlearium* metabolites from both intracellular and extra-cellular content. The digestive

process of mice could lead to bacterial cell degradation and the release of its cellular components and intracellular metabolites, which other native bacteria could utilize these for survival or other functionality.

CHAPTER 4. DETERMINE THE POTENTIAL MECHANISM BASED ON GUT MICROBIOME

The 16S rRNA sequencing data has proved the significant separation between the HF and CC groups' gut communities. To better explore the 16S sequences and understand the gut microbiome, functional gene analysis was performed. The Phylogenetic Investigation of Communities by Reconstruction of Unobserved States (PICRUST2) was used to support the prediction of characterization in a community of organisms. The gene family abundance was predicted in environmental DNA samples for the 16S rRNA gene [148]. After identifying the gene from 16S rRNA, the abundance of functional genes, specifically enzymes, were predicted. Subsequently, the predicted enzymes were regrouped to the MetaCyc reactions database to predict MetaCyc pathway abundances. The pathway abundances would uncover the potential mechanism between the gut microbiome and changed phenotypes. In this investigation, the enzymes from bacteria and bacteria-participated pathways were predicted. It was hypothesized that the increasing SCFAs-related enzymes and pathways abundance would be shown in the *C. cochlearium* treated group.

Methods

Functional gene analysis

The Greengenes close-reference OTU table computed by Qiime2 was prepared for further analysis. The pipeline called PICRUST2 (Version 2.3.0 beta) was utilized in this study to predict the enrichment of functional genes in the gut microbiome of the HF and CC groups based on marker gene sequences from 16S sequencing data and a database of reference genomes [148-151]. Enzyme Classification (EC) numbers were first predicted through the hidden state prediction [152]. The MetaCyc reactions prediction was based on the abundance of EC number prediction after

reorganizing them into MetaCyc pathways. Likewise, the presence of minimum pathways in accordance with the presence of gene families was identified by MinPath [153]. The GraphPad Prism (V 7.0, La Jolla, CA) was performed to further analyze and visualize the output of PICRUSt2 results.

Short-chain fatty acids measurement

The intestinal content of each mouse was sampled and pooled by group. After homogenizing the pooled samples, two aliquots per group were prepared for further measurement. SCFAs, including acetate, including propionate, and butyrate, were derivatized with a propyl chloroformate/pyridine mixture. Samples were then examined using gas chromatography-mass spectrometry (GC-MS) based on the previously published method [154, 155]. The retention times for different metabolites were varied. For acetate, the retention time was 2.119 min, while the retention time of propionate was 3.309 min. The retention time of butyrate was the longest among the three, which was 4.741 min. The quantitative ions for acetate, propionate, and butyrate were varied as well, which were m/z 61, 75, and 71, respectively.

RNA extraction

The liver and intestine tissue RNA were extracted using the Invitrogen™ PureLink™ RNeasy Mini Kit (Carlsbad, CA) following the manufacturer's protocol. Tissues were brought from a -80 °C freezer and placed on the ice to obtain the correct sample weight. The rotor-stator homogenizer was used to homogenize the sample with the fresh lysis buffer. Samples were then centrifuged, and the supernatant was transferred to a clean RNase-free tube. The 100% ethanol was added to the supernatant, and then the supernatant was transferred to the spin cartridge to bind, wash, and elute RNA. The eluted RNA samples from the supernatant were further analyzed for

the quality and quantity by the Thermo Scientific™ NanoDrop 2000 spectrophotometer (Wilmington, DE). The RNA samples were stored at -80 °C for future analysis.

Reverse transcription-quantitative polymerase chain reaction (RT-PCR)

The RNA samples were reverse transcribed to cDNA by using the iScript™ Reverse Transcription Supermix (Hercules, CA). The Bio-rad CFX Connect real-time PCR instruments (Hercules, CA) was used for running RT-PCR. The NanoDrop 2000 spectrophotometer was used to evaluate the cDNA concentration.

Real-time quantitative polymerase chain reaction (qPCR/real-time PCR)

Targeted Gene-specific primers were used, and all the results were normalized with the housekeeping gene of GAPDH. iTaq Universal SYBR Green Supermix (Hercules, CA) solution was used as the real-time PCR reagents, which is 2× concentrated. The Bio-rad CFX Connect real-time PCR instruments were used for running the qPCR, in which real-time PCR data were collected and evaluated by the CFX Maestro Software (Hercules, CA). Duplication was performed for each sample. The relative gene expressions were calculated by the Livak/delta delta Ct method [156, 157]. Primer sequences are presented in **Table 7**.

Statistical analysis

Data were analyzed and presented as means \pm SEM. The functional gene results and gene expression between the HF and CC groups were performed using the Student t-test with GraphPad Prism (V 7.0, La Jolla, CA). The Person correlation coefficients were computed to analyze the correlation between body weight and the predicted enzymes or pathways, combining both the HF and CC groups' data. The SCFAs concentration among the LF, HF, and CC groups was analyzed using one-way ANOVA and followed by a post-hoc for multiple comparisons with GraphPad Prism. Results were considered statistically significant at $P < 0.05$.

Results

PICRUSt2 was performed as the functional gene analysis. The hidden-state prediction of the enzymes was first computed. There were 1,684 enzymes/functional genes predicted based on the 16S sequencing data. Among them, 974 enzymes showed a significant difference between the HF and CC groups. The abundance of 14 selected SCFAs-related enzymes or functional genes among the HF and CC groups is displayed in **Table 8**. The correlations between body weight and these enzymes are shown in **Table 9**. The abundance of all the SCFAs-related enzymes was elevated in the CC group when compared to the HF group, except for propionate kinase (Enzyme Commission (EC): 2.7.2.15). All the four butyrate-producing enzymes, including phosphate butyryltransferase (EC: 2.3.1.19), butyrate kinase (EC: 2.7.2.7), acetate CoA-transferase (EC: 2.8.3.8), and short-chain acyl-CoA dehydrogenase (EC: 1.3.8.1), were significantly elevated in the CC group when compared to the HF group (**Table 8**). However, according to the correlation results (**Table 9**), only acetate CoA-transferase was shown to be inversely correlated with the host's body weight ($P < 0.01$). The phosphate butyryltransferase and short-chain acyl-CoA dehydrogenase had a trend of negative correlation with body weight but the relationships failed to be significant ($P > 0.05$). For other SCFAs-related enzymes, phosphate acetyltransferase ($P < 0.01$), acetate--CoA ligase ($P < 0.01$), propionate--CoA ligase ($P < 0.05$), propionate CoA-transferase ($P < 0.0001$), and propionyl-CoA carboxylase ($P < 0.05$), the significantly differential abundance between the HF and CC groups was observed (**Table 8**). Among these, propionate--CoA ligase, propionate CoA-transferase, and propionyl-CoA carboxylase showed significant inverse correlations between body weight and concentration of these enzymes. Additionally, there were two functional genes, succinyl-CoA: acetate CoA-transferase ($P = 0.051$) and urocanate reductase ($P = 0.063$), showing the trend to significantly increase the abundance in the CC group compared to the HF group.

The predicted pathway analyzed by PICRUST2 was anticipated based on the abundance of functional genes/enzymes. In total, 326 pathways involved with those enzymes were predicted. Among these, the significant differences between the HF and CC groups were observed in 194 pathways by Student t-test. Thirteen SCFAs-related pathways were chosen for analyzing the SCFAs metabolism through gut microbiota. The abundance of SCFAs-related pathways is demonstrated in **Table 10**, while the correlation of these pathways was further investigated and is presented in **Table 11**. Six butyrate-related pathways were predicted, which are butyrate-producing pathways through gut bacteria. Among these, the abundance of five pathways, including acetyl-CoA fermentation to butanoate II ($P < 0.0001$), pyruvate fermentation to butanoate ($P < 0.001$), L-lysine fermentation to acetate and butanoate ($P < 0.0001$), L-glutamate degradation V (via hydroxyglutarate) ($P < 0.01$), and succinate fermentation to butanoate ($P < 0.05$) were significantly higher in the CC group compared to the HF group. Three out of the five pathways, acetyl-CoA fermentation to butanoate II ($r = -0.55$, $P < 0.01$), pyruvate fermentation to butanoate ($r = -0.52$, $P < 0.05$), and L-lysine fermentation to acetate and butanoate ($r = -0.55$, $P < 0.01$), was inversely correlated with body weight, while the abundance of L-glutamate degradation V (via hydroxyglutarate) had a trend to be negatively correlated with body weight ($P = 0.074$). Additionally, 6 acetate-related pathways were chosen for investigation in this study, including L-lysine fermentation to acetate and butanoate, pyruvate fermentation to acetate and lactate II, pyruvate fermentation to acetone, hexitol fermentation to lactate, formate, ethanol, and acetate, methanogenesis from acetate, and TCA cycle VII (acetate-producers). Among these, the L-lysine fermentation to acetate and butanoate, which is mentioned above, has been linked to both acetate and butyrate production. Among other five acetate-related pathways, three of them, pyruvate fermentation to acetate and lactate II ($P < 0.05$), pyruvate fermentation to acetone ($P < 0.0001$),

and hexitol fermentation to lactate, formate, ethanol, and acetate ($P < 0.05$), have shown a significantly differential abundance between the HF and CC groups. Among these, only the pathway of pyruvate fermentation to acetone is the acetate-degradation pathway, while the other two pathways are acetate-producing. Remarkably, the abundance of pyruvate fermentation to acetate and lactate II, and pyruvate fermentation to acetone pathways were significantly elevated in the CC group, while the abundance of hexitol fermentation to lactate, formate, ethanol and acetate pathway revealed a significant decrease in the CC group when compared to the HF group. Among the three significantly shifted pathways, two of them have been significantly linked with body weight in the opposite direction. The pathway of pyruvate fermentation to acetone has been negatively correlated with body weight ($r = -0.51$, $P < 0.05$), while the pathway of hexitol fermentation to lactate, formate, ethanol and acetate indicated the positive correlation with body weight ($r = 0.49$, $P < 0.05$). Likewise, there are two propionate-related pathways selected in this investigation, including pyruvate fermentation to propanoate I and L-glutamate degradation VIII (to propanoate), which produce propionate through gut microbiota. Among two propionate-related pathways, only the pathway of pyruvate fermentation to propanoate I revealed a significant increase in the CC group ($P < 0.05$) when compared to the HF group. Analyzed by the Pearson correlation coefficient, a negative correlation trend was observed between the abundance of pyruvate fermentation to propanoate I pathway and body weight ($r = -0.41$, $P = 0.06$).

The SCFAs metabolites were measured from the intestinal content using GC-MS, including the acetate, propionate, and butyrate. All the intestinal contents from each mouse were gathered and pooled by group. The grouped samples were homogenized, and duplicated samples were measured. The metabolites concentrations are presented in **Table 12**. The acetate level in the HF group was significantly higher than in the LF and CC groups. The acetate concentration in the

CC group was significantly increased compared to the LF group as well ($P < 0.001$). Additionally, the CC group had the highest propionate level among the three groups. The propionate concentration in the CC group was significantly higher than that of the HF group ($P < 0.01$). The trend of butyrate concentration results was similar to the trend of acetate level among the three groups. The HF group had the highest level of butyrate concentration among the three groups, which was significantly different from that of the CC group ($P < 0.0001$). A significant difference in butyrate level was also observed between the LF and CC groups, with the level of the CC group higher than that of the LF group ($P < 0.01$).

The real-time PCR was performed to evaluate the SCFAs-related gene expression, including *ffar2*, *ffar3*, *HCAR2*, *SLC16A1*, and *SLC5A8*. Free fatty acid receptor 2 (FFAR2) (GPR43), FFAR3 (GPR41), and GPR109A (encoded by *HCAR2* gene) are the G protein-coupled receptors (GPRs) of SCFAs, while MCT1 (encoded by *SLC16A1* gene) and SMCT1 (encoded by *SLC5A8* gene) are the transporters of SCFAs [158]. The intestinal RNA of each mouse was first extracted and then reverse transcribed to cDNA. The intestinal cDNA was utilized to estimate the gene expression of *ffar2*, *ffar3*, *HCAR2*, *SLC16A1*, and *SLC5A8*. At the same time, the liver RNA was also extracted and reverse transcribed to cDNA. The gene expression of *ffar2*, *ffar3* and *HCAR2* was measured for liver cDNA, which are the receptors of SCFAs in liver tissue [159]. According to our relative normalized expression results from intestinal cDNA shown in **Figure 15-19**, only the *ffar2* gene had a significant difference between the HF and CC group ($P < 0.0001$), which was significantly downregulated in the CC group. However, no significant difference among the HF and CC groups was observed in the *ffar2* gene expression from liver cDNA (**Figure 20**). Besides, *ffar3* and *HCAR2* genes extracted from liver tissue also showed no difference between the HF and CC groups (**Figure 21** and **Figure 22**).

Discussion

The functional genes/enzymes and pathways were predicted through PICRUST2 based on the 16S rRNA sequencing results. Since the modulation of gut microbial composition was detected, the changes between the HF and CC groups were discovered, indicating that the increase of SCFAs-producing bacteria strongly contributed to the gut microbiome composition of the CC group. Thus, the SCFAs-related enzymes and pathways, especially the SCFAs synthesis pathways, require further investigation.

According to the metabolic routes for butyrate production, there are direct and indirect pathways for butyrate synthesis [121]. The direct pathway converts carbohydrate directly to butyrate through butyrate kinase (EC: 2.7.2.7), while the indirect pathways synthesize butyrate from acetate via butyryl-CoA: acetate CoA transferase (EC: 2.8.3.8), succinate through succinyl-CoA synthetase and lactate by lactate dehydrogenase, and finally via butyrate kinase as shown in **Figure 23** [121, 160]. Thus, the genes of butyryl-CoA: acetate CoA transferase and butyrate kinase have been utilized as biomarkers for detecting the butyrate-producing microbiome. Additionally, we analyzed another two enzymes, short-chain acyl-CoA dehydrogenase/butyryl-CoA dehydrogenase (EC: 1.3.8.1) and phosphate butyryltransferase/phosphotransbutyrylase (EC: 2.3.1.19), both involved in the pathways for butyrate production. All four of them showed a significant increase in the CC group compared to the HF group, suggesting an elevated butyrate production in the gut via the microbiota in the CC group. Interestingly, when correlation analyses were conducted, only acetate CoA-transferase showed a significantly negative correlation with body weight, which indicated the acetate CoA-transferase could be linked with the anti-obesity effect of *C. cochlearium* supplementation. Furthermore, the acetate CoA-transferase-involved pathway, acetyl-CoA fermentation to butanoate II, showed a significant difference between the

HF and CC groups. The abundance of this pathway in the CC group was elevated by 105.0% compared to that of the HF group, which means the abundance in the CC group was more than twice the abundance in the HF group. Moreover, the pathway has been shown to be negatively correlated with body weight in accordance with Pearson's correlation test. It was suggested that the abundance of acetyl-CoA fermentation to butanoate II pathway could be used as the obesity indicator, the higher abundance meaning the lower body weight. The majority of butyrate-producing pathways depicted in **Figure 23** were detected in the functional gene analysis in terms of the abundance of enzymes, except the lactate to butyrate pathway, which can be combined with pyruvate to butyrate pathway. However, not all of the six butyrate-producing pathways discovered by the PICRUST2 were significantly different between the two groups. Apart from the acetyl-CoA fermentation to butanoate II, four pathways of pyruvate fermentation to butanoate, L-lysine fermentation to acetate and butanoate, L-glutamate degradation V (via hydroxyglutarate), and succinate fermentation to butanoate were significantly elevated in the CC group compared to the HF group, which suggested that the administration of *C. cochlearium* promoted the butyrate-producing pathways by modulating the gut microbiome. Among these, the pathway of pyruvate fermentation to butanoate and the pathway of L-lysine fermentation to acetate was negatively correlated with body weight, indicating that the increasing abundance of butyrate-producing pathways bacteria by *C. cochlearium* supplementation has been linked to the anti-obesity effect. In other words, the mechanism of the probiotic effect of *C. cochlearium* supplementation could be through increasing butyrate-producing bacteria and their participation of butyrate-producing pathways and consequently elevating the butyrate level in the gut and resulting in an anti-obesity activity. Thus, the synthesized butyrate in the intestine would be the key to explaining this mechanism.

Acetate- and propionate-related enzymes and pathways were also analyzed. There are two acetate-related enzymes showing significant elevation in the CC group. These were phosphate acetyltransferase and acetate--CoA ligase, although there was no correlation between these two enzymes and body weight. Both of them participated in pathways of acetate degradation, while the acetate--CoA ligase participated in a reversible reaction between acetate and acetate-CoA. Three pathways involved with acetate production showed a significant difference, in which pathways of pyruvate fermentation to acetate and lactate II and pyruvate fermentation to acetone were increased in the CC group while the abundance of the pathway hexitol fermentation to lactate, formate, ethanol and acetate was reduced as compared to the HF group. Considering Pearson's correlations, pathways of pyruvate fermentation to acetone and hexitol fermentation to lactate, formate, ethanol, and acetate were correlated with body weight in reverse regulation. It is challenging to predict acetate production levels because acetate is not only the end-product but also the co-substrate for other pathways working as a regulator [161]. Thus, the status of acetate production cannot be predicted and concluded.

Three enzymes involved with propionate pathways were significantly increased in the CC group relative to the HF group, and these were propionate--CoA ligase, propionate CoA-transferase, and propionyl-CoA carboxylase. All of them have been inversely correlated with body weight. Actually, these three enzymes participated in the propionate degradation pathways. Among these, the enzyme of propionate--CoA ligase was not a good prediction of propionate metabolism due to the small abundance in both the HF and CC groups. Analyzing the predicted pathway, pyruvate fermentation to propanoate I pathway was significantly elevated abundance in the CC group as compared to the HF group, and with a trend of negative correlation with obesity.

Thus, the propionate production in the intestine of the CC group was expected to increase, which was modulated by *C. cochlearium* administration.

It was hypothesized that the higher butyrate level would be observed in the CC group due to *C. cochlearium* supplementation and the increase of other butyrate-producing bacteria. However, the butyrate concentration in the intestinal content was significantly lower in the CC group than in the HF group, which was against our hypothesis. Not only butyrate concentration but also acetate concentration was significantly higher in the HF group compared to the CC group. Nevertheless, the propionate concentration in the CC group was the highest among the three groups. Similar to our findings, an animal study conducted by Turnbaugh et al. observed the increased butyrate ($P < 0.01$) and acetate ($P < 0.01$) in cecum from obese *ob/ob* mice relative to their lean counterparts [38]. Numerous human studies had similar results indicating that an elevated SCFAs level in feces has been detected in obese individuals relative to their lean individuals, and these elevated SCFAs have been associated with obesity, gut dysbiosis, and hypertension [131, 162, 163]. There is no doubt that the SCFAs have been widely considered as beneficial metabolites [164, 165]. Studies on the circulating SCFAs levels indicated an inverse association with blood pressure, insulin resistance, and obesity [166, 167]. There is no association between fecal acetate and butyrate levels and their respective circulating concentration; however, the circulating propionate level was positively correlated with fecal propionate concentration [167]. It is consistent with our findings that the propionate concentration in the intestinal content was significantly higher in the CC group than in the HF group, which suggested the high circulating propionate concentration in CC mice. It was suspected that the reduced level of SCFAs in the CC group was due to the fact that SCFAs were absorbed and utilized by the host quickly, whereas the transient change of SCFAs

concentration is hard to detect [168]. Thus, a more sensitive method for the timely detection of SCFAs is needed in future studies.

However, studies have shown that SCFAs could modulate the host's phenotype through endothelial GPRs [166]. The real-time PCR was performed to measure the gene expression of SCFAs-related receptors and transporters. The downregulation of the *ffar2* gene was found in the investigation. FFAR2 (GPR43) has been reported as the receptor of acetate, propionate, and butyrate, and is able to be activated by SCFAs [169]. The *ffar2* gene is highly expressed in the intestinal epithelium and the immune cells [158]. It is inconsistent that the downstream *ffar2* was revealed when the increasing butyrate-producing bacteria and pathways were predicted. Additionally, there is no significant difference in the gene expression of the other receptors and transporters in both liver and intestine tissues. Long-term fasting and change of circadian rhythm of the mice could impact acute liver SCFAs metabolism and its related genes in C57BL/6 mice [170, 171]. This could also impact the intestinal SCFAs metabolism. Therefore, further investigation is needed to measure the gene expression of SCFAs-related receptors and transporters without the factor of fasting.

Conclusion

There are limited studies on the health effects of *C. cochlearium*. As a butyrate producer, *C. cochlearium* could have a potential probiotic effect against obesity. After 16 weeks of high-fat diet treatment supplemented with *C. cochlearium*, the CC group had significantly lower body weight gain, fat mass, and fat/lean ratio than the HF group without a change in lean mass. Moreover, the energy expenditure of BMR and activity level significantly increased, indicating the elevation of fat oxidation. This suggested that the administration of *C. cochlearium* had the ability to attenuate body weight gain by reducing the fat mass through fat oxidation. Furthermore, the

glucose homeostasis was also improved with *C. cochlearium* supplementation, including fasting blood glucose, glucose tolerance, fasting insulin, and HOMA-IR. The 16S rRNA sequencing data revealed a significant microbial separation between the HF and CC groups in alpha- and beta-diversity analyses. The F/B ratio significantly decreased from 4.91 in the HF group to 3.54 in the CC group, which has been positively associated with body weight. Based on the LEfSe analysis, the families of *Christensenellaceae* and *Lachnospiraceae*, *Mogibacteriaceae*, *Rikenellaceae*, and *S24_7* have been detected as a significant contribution to the CC group, and these families have been inversely associated with body weight. Among these, the families of *Christensenellaceae* and *Lachnospiraceae* are SCFAs-producing bacteria. On the contrary, the increased abundance of families *Streptococcaceae* and *Lactobacillaceae* in the HF group have been correlated with obesity. It can be concluded that *C. cochlearium* supplementation had a beneficial effect against obesity through increasing anti-obesity-related bacteria, especially SCFAs-producing bacteria, and decreasing obesity-related taxa. Further functional gene analysis has confirmed that the administration of *C. cochlearium* increased the butyrate-producing enzymes and pathways, and propionate-related pathways. Thus, the administration of *C. cochlearium* promoted SCFAs production, especially butyrate production, and subsequently exert the anti-obesity effect. In this case, the reduced body weight gain, elevated resting energy expenditure and activity level, and improved insulin sensitivity can be at least partly explained by the increasing butyrate production. Nevertheless, the concentration of butyrate and acetate in the intestinal content was significantly lower in the CC group relative to the HF group, which was consistent with previous studies indicating that the fecal and cecal SCFAs levels were associated with obesity [131, 162, 163]. Additionally, there is no significant difference in the gene expression of SCFAs receptors and

transporters, except for the abnormal *ffar2* gene. These abnormal gene expression results might be impacted by the long fasting time before euthanasia.

Future direction

In the current study, the supplementation of *C. cochlearium* showed a significantly reduced weight gain and improved insulin sensitivity compared to the HF group. However, *C. cochlearium* was not observed in the OTU table from the 16s rRNA sequencing performed, which could be categorized into unclassified bacteria. In future studies, those unclassified bacteria need to be identified. The NCBI taxonomy database, which is more comprehensive than the Greengenes database and updated daily, could be an alternative to identify those unclassified bacteria via blasting those unidentified sequences. Additionally, it would also be interesting to conduct another animal study with heat-treated *C. cochlearium* supplementation as a comparison, which could lead to further understanding other potential mechanisms of its effect on the changes in the gut microbiome that may lead to preventing obesity. Previous studies have stated that some probiotics, either in live or dead forms, may have a beneficial effect on preventing obesity and metabolic syndromes [172, 173]. With the comparison of heat-killed *C. cochlearium* administration, we can clarify whether there would be additional cellular components or metabolites that lead to change in microbial interactions.

Moreover, significant elevations of butyrate and acetate concentrations were observed in obese HF mice rather than the CC mice. Although it is consistent with previous findings, it is suspected that butyrate and acetate have been quickly absorbed and utilized by hosts. Thus, it is necessary to detect circulating SCFAs to evaluate the reaction between SCFAs and the host. It is hypothesized that the circulating SCFAs are significantly elevated with *C. cochlearium* supplementation, which would suggest the increased utilization of SCFAs by the CC host.

Furthermore, the measurement of circulating SCFAs should be conducted on both the fed and fasting states, and this may reduce the interference of food availability to SCFAs utilization. In addition, the SCFAs receptors and transporter in both the liver and intestine tissue should be estimated on fed status instead of fasting, which could help to depict the interaction between SCFAs and the host. Similarly, the specific pathway involved in the utilization of SCFAs by the host could be further studied to understand increased fat oxidation and physical activity.

In this investigation, the administration of *C. cochlearium* showed the probiotic effect on a high-fat diet-induced obesity model. However, probiotics are usually taken by people who are looking for alternative methods to lose weight. Thus, it is important to explore the effect of *C. cochlearium* after the onset of obesity, which is highly individualized in severity. It is warranted to consider the modification of dosage or frequency of *C. cochlearium* administration. Since the developed obese model has a higher body weight than the inducing model, the dosage needs to be increased based on the body weight. It would be informative to conduct the dose-response experiments of *C. cochlearium* to acquire the most efficient dosage for the developed obese model.

TABLES AND FIGURES

Table 1. Nutrient composition and caloric content of the Low-fat Diet (LF) and the High-fat Diet (HF) used in the experiment

Ingredient	LF (D12450J)		HF (D12492M)	
	gm	kcal	gm	kcal
Casein, 30 Mesh	200	800	200	800
L-Cystine	3	12	3	12
Corn Starch	506.2	2024.8	0	0
Maltodextrin 10	125	500	125	500
Sucrose	68.8	275.2	68.8	275
Cellulose, BW200	50	0	50	0
Soybean Oil	25	225	25	225
Lard	20	180	245	2205
Mineral Mix S10026	10	0	10	0
DiCalcium Phosphate	13	0	13	0
Calcium Carbonate	5.5	0	5.5	0
Potassium Citrate, 1 H ₂ O	16.5	0	16.5	0
Vitamin Mix V10001	10	40	10	40
Choline Bitartrate	2	0	2	0
Overall	gm%	kcal%	gm%	kcal%
Protein	19.2	20	26	20
Carbohydrate	67.3	70	26	20
Fat	4.3	10	35	60
Total		100		100
kcal/gm	3.85		5.24	

Table 2. Biometrics results in the LF, HF and CC groups at 16 weeks

	Group			P value		
	LF	HF	CC	ANOVA	HF vs. CC	LF vs. CC
Body weight, g	30.5 ± 0.8	50.2 ± 0.7	43.7 ± 1.2	<0.0001	<0.0001	<0.0001
Percentage weight gain, %	36.1 ± 2.9	101.4 ± 3.1	85.6 ± 5.4	<0.0001	0.0002	<0.0001
Fat mass, g	5.7 ± 0.6	22.9 ± 0.6	17.3 ± 0.7	<0.0001	<0.0001	<0.0001
Percentage fat, %	19.4 ± 2.1	47.1 ± 0.8	41.7 ± 0.8	<0.0001	0.0230	<0.0001
Lean mass, g	20.0 ± 0.9	21.2 ± 0.4	19.2 ± 0.4	0.0974	0.0615	0.5763
Percentage lean, %	70.0 ± 2.1	43.7 ± 0.7	46.4 ± 0.9	<0.0001	0.3319	<0.0001
Fat/Lean ratio	0.3 ± 0.0	1.1 ± 0.0	0.9 ± 0.0	<0.0001	0.0033	<0.0001

Values are means ± SEM (n = 12 per group). The statistical significance was calculated at P < 0.05.

Table 3. Blood biochemistry results in the LF, HF and CC groups at 16 weeks

	Group			P value		
	LF	HF	CC	ANOVA	HF vs. CC	LF vs. CC
Fasting Glucose, mg/dL	162.6 ± 9.5	223.8 ± 14.5	175.2 ± 10.3	0.0017	0.0121	0.6717
Fasting Insulin, mU/L	49.5 ± 5.5	192.4 ± 13.8	121.5 ± 16.3	<0.0001	0.0017	0.0011
HOMA-IR	19.4 ± 2.4	104.8 ± 13.2	55.3 ± 10.5	<0.0001	0.0031	0.0236

Values are means ± SEM (n = 8-10 per group). The statistical significance was calculated at P < 0.05.

Table 4. Energy balance results in the LF, HF and CC groups

	Group			P value	HF vs. CC	LF vs. CC
	LF	HF	CC			
Food intake, kcal/day/mouse	10.4 ± 0.2	11.4 ± 0.4	10.7 ± 0.3	0.6500	0.8596	0.9001
Fecal energy, kcal/day/mouse	0.8 ± 0.0	1.3 ± 0.0	1.1 ± 0.0	<0.0001	<0.0001	<0.0001
Calorie absorption, kcal/day/mouse	9.4 ± 0.0	9.6 ± 0.0	10.1 ± 0.0	<0.0001	<0.0001	<0.0001
Feed efficiency, %	0.7 ± 0.1	2.0 ± 0.1	1.7 ± 0.1	<0.0001	0.0074	<0.0001

Values are means ± SEM (n = 12 per group). The statistical significance was calculated at P < 0.05.

Table 5. Metabolic results in the LF, HF and CC groups at 16 weeks

	Group		P value
	HF	CC	HF vs. CC
RER	0.777 ± 0.004	0.791 ± 0.004	0.0398
BMR, kcal/day/kg	212.2 ± 5.8	234.9 ± 6.7	0.0182
Distance traveled, m/day	1103.8 ± 135.6	2003.2 ± 417.1	0.0390

Values are means ± SEM (n = 12 per group). The statistical significance was calculated at P < 0.05.

Table 6. Relative abundance of phylum classification in the HF and CC groups

Phylum	HF	CC	P value
Acidobacteria	0.0 ± 0.0 %	0.0 ± 0.0 %	0.3741
Actinobacteria	1.0 ± 0.1 %	1.2 ± 0.3 %	0.5076
Bacteroidetes	16.5 ± 1.6 %	21.3 ± 1.8 %	0.0680
Chlorobi	0.0 ± 0.0 %	0.0 ± 0.0 %	0.2840
Deferribacteres	2.7 ± 0.5 %	2.9 ± 0.4 %	0.7889
Firmicutes	74.4 ± 1.6 %	67.6 ± 1.9 %	0.0114
Proteobacteria	4.5 ± 0.5 %	6.3 ± 0.4 %	0.0185
TM7	0.1 ± 0.0 %	0.0 ± 0.0 %	0.2903
Tenericutes	0.1 ± 0.0 %	0.0 ± 0.0 %	0.0006
Verrucomicrobia	0.7 ± 0.2 %	0.7 ± 0.2 %	0.8850
Unclassified	0.0 ± 0.0 %	0.0 ± 0.0 %	0.7302
Firmicutes/Bacteroidetes ratio	4.9 ± 0.4	3.5 ± 0.5	0.0409

Values are mean ± SEM (n = 10 per group). The statistical significance was calculated at P < 0.05.

Table 7. Primers for real-time PCR

Gene	Primer	
	Forward	Reverse
<i>GAPDH</i>	CAAGGAGTAAGAAACCCTGGACC	CGAGTTGGGATAGGGCCTCT
<i>ffar2</i>	CTTGATCCTCACGGCCTACAT	CCAGGGTCAGATTAAGCAGGAG
<i>ffar3</i>	CTTCTTTCTTGGCAATTACTGGC	CCGAAATGGTCAGGTTTAGCAA
<i>HCAR2</i>	GGGGCTGGAATTTGTGTTCG	ATGAAGAGCATCACACGGCA
<i>SLC16A1</i>	TGTTAGTCGGAGCCTTCATTTC	CACTGGTCGTTGCACTGAATA
<i>SLC5A8</i>	CGGGACATCGGCAGTTTTG	CTGCGACCGCCCATAAGAA

Table 8. SCFAs-related predicted enzymes between the HF and CC groups

	Group		P value
	HF	CC	HF vs. CC
Phosphate butyryltransferase ¹	21682.5 ± 3044.4	38017.5 ± 3229.5	0.0015
Butyrate kinase ¹	24096.6 ± 3461.7	43956.2 ± 4441.3	0.0019
Acetate CoA-transferase ¹	12138.9 ± 1549.1	26762.5 ± 1461.7	<0.0001
Short-chain acyl-CoA dehydrogenase ¹	13314.1 ± 1826.6	29533.0 ± 3215.7	0.0002
Acetate kinase ²	76564.8 ± 10877.7	88338.7 ± 8417.1	0.4168
Acetoacetate decarboxylase ²	0.3 ± 0.3	0.0 ± 0.0	0.3741
Phosphate acetyltransferase ³	69174.4 ± 9422.5	114670.4 ± 11589.7	0.0059
Acetate--CoA ligase ^{2,3}	14110.4 ± 2496.8	23300.3 ± 1728.4	0.0088
Succinyl-CoA:acetate CoA-transferase ³	114.4 ± 47.8	5.2 ± 2.2	0.0511
Propionate kinase ⁴	154.9 ± 38.6	76.8 ± 32.5	0.1467
Urocanate reductase ⁴	348.8 ± 51.4	645.90 ± 153.7	0.0626
Propionate--CoA ligase ^{4,5}	0.0 ± 0.0	4.3 ± 1.9	0.0244
Propionate CoA-transferase ⁵	7568.3 ± 1086.7	18166.5 ± 1224.1	<0.0001
Propionyl-CoA carboxylase ⁵	8046.5 ± 1582.5	13656.9 ± 1498.5	0.0195

Values are mean ± SEM (n = 10 per group). ¹: are butyrate-producing enzymes, ²: acetate-producing enzymes, ³: acetate-degradation enzymes, ⁴: propionate-producing enzymes, ⁵: propionate-degradation enzymes. The statistical significance was calculated at P < 0.05.

Table 9. Correlation between body weight and SCFAs-related predicted enzymes

	Correlation	P value
Phosphate butyryltransferase ¹	-0.38	0.082
Butyrate kinase ¹	-0.34	0.121
Acetate CoA-transferase ¹	-0.54	0.009
Short-chain acyl-CoA dehydrogenase ¹	-0.39	0.069
Acetate kinase ²	0.02	0.923
Acetoacetate decarboxylase ²	0.25	0.252
Phosphate acetyltransferase ³	-0.27	0.224
Acetate--CoA ligase ^{2,3}	-0.40	0.068
Succinyl-CoA:acetate CoA-transferase ³	0.33	0.130
Propionate kinase ⁴	0.31	0.162
Urocanate reductase ⁴	-0.08	0.735
Propionate--CoA ligase ^{4,5}	-0.54	0.009
Propionate CoA-transferase ⁵	-0.51	0.016
Propionyl-CoA carboxylase ⁵	-0.45	0.034

Values are mean \pm SEM (n = 10 per group). ¹: butyrate-producing enzymes, ²: acetate-producing enzymes, ³: acetate-degradation enzymes, ⁴: propionate-producing enzymes, ⁵: propionate-degradation enzymes. The statistical significance was calculated at P < 0.05.

Table 10. SCFAs-related predicted pathways between the HF and CC groups

	Group		P value
	HF	CC	HF vs. CC
acetyl-CoA fermentation to butanoate II ¹	17590.3 ± 2124.5	36060.3 ± 1901.6	<0.0001
pyruvate fermentation to butanoate ¹	5145.0 ± 607.1	8733.8 ± 565.9	0.0003
L-lysine fermentation to acetate and butanoate ^{1,2}	3637.3 ± 456.8	7001.8 ± 352.7	<0.0001
4-aminobutanoate degradation V ¹	5530.1 ± 745.8	4311.2 ± 566.9	0.2232
L-glutamate degradation V (via hydroxyglutarate) ¹	3303.0 ± 403.3	6399.5 ± 806.7	0.0017
succinate fermentation to butanoate ¹	132.3 ± 53.1	999.3 ± 362.4	0.0174
pyruvate fermentation to acetate and lactate II ²	69915.7 ± 9469.3	102113.3 ± 9601.8	0.0280
hexitol fermentation to lactate, formate, ethanol and acetate ²	14954.5 ± 2014.7	8725.8 ± 1303.0	0.0222
TCA cycle VII (acetate-producers) ²	1615.6 ± 449.6	1087.9 ± 200.9	0.3287
pyruvate fermentation to acetone ³	19008.6 ± 2419.9	40783.1 ± 2435.3	<0.0001
methanogenesis from acetate ³	2263.7 ± 413.1	2371.7 ± 260.9	0.8352
pyruvate fermentation to propanoate I ⁴	25597.7 ± 4820.4	41845.7 ± 2959.3	0.0128
L-glutamate degradation VIII (to propanoate) ⁴	451.8 ± 110.8	267.3 ± 108.9	0.2538

Values are mean ± SEM (n = 10 per group). ¹: butyrate-producing pathways, ²: acetate-producing pathways, ³: acetate-degradation pathways, ⁴: propanoate-producing pathways. The statistical significance was calculated at P < 0.05.

Table 11. Correlation between body weight and SCFAs-related predicted pathways

	Correlation	P value
acetyl-CoA fermentation to butanoate II ¹	-0.55	0.008
pyruvate fermentation to butanoate ¹	-0.52	0.014
L-lysine fermentation to acetate and butanoate ^{1,2}	-0.55	0.008
4-aminobutanoate degradation V ¹	-0.21	0.260
L-glutamate degradation V (via hydroxyglutarate) ¹	-0.39	0.074
succinate fermentation to butanoate ¹	0.25	0.346
pyruvate fermentation to acetate and lactate II ²	-0.20	0.374
hexitol fermentation to lactate, formate, ethanol and acetate ²	0.49	0.021
TCA cycle VII (acetate-producers) ²	0.06	0.786
pyruvate fermentation to acetone ³	-0.51	0.015
methanogenesis from acetate ³	-0.10	0.645
pyruvate fermentation to propanoate I ⁴	-0.41	0.060
L-glutamate degradation VIII (to propanoate) ⁴	0.33	0.140

Values are mean \pm SEM (n = 10 per group). ¹: butyrate-producing pathways, ²: acetate-producing pathways, ³: acetate-degradation pathways, ⁴: propanoate-producing pathways. The statistical significance was calculated at $P < 0.05$.

Table 12. SCFAs concentration in intestinal content between the HF and CC groups

	Group			P value		
	LF	HF	CC	ANOVA	HF vs. CC	LF vs. CC
Acetate, $\mu\text{mol/g}$	58.1 ± 1.0	96.9 ± 0.4	82.6 ± 0.9	<0.0001	0.0009	0.0001
Propionate, $\mu\text{mol/g}$	3.6 ± 0.6	5.0 ± 0.5	9.2 ± 0.5	0.0035	0.0080	0.0035
Butyrate, $\mu\text{mol/g}$	5.0 ± 0.1	13.4 ± 0.2	7.4 ± 0.1	<0.0001	<0.0001	0.0014

Values are mean \pm SEM (n = 12 per group). The statistical significance was calculated at P < 0.05.

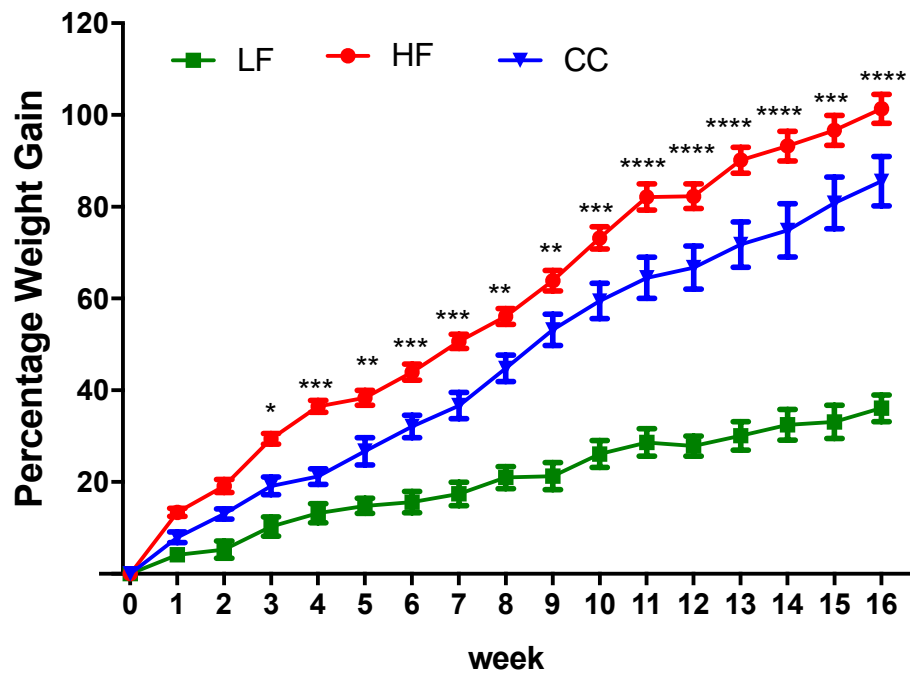


Figure 1. Average percentage body weight gain over a 16-week period

Values are means \pm SEM, $n = 12$. * $P < 0.05$, ** $P < 0.01$, *** $P < 0.001$, and **** $P < 0.0001$ indicating significant difference between the HF and CC groups for weekly body weight.

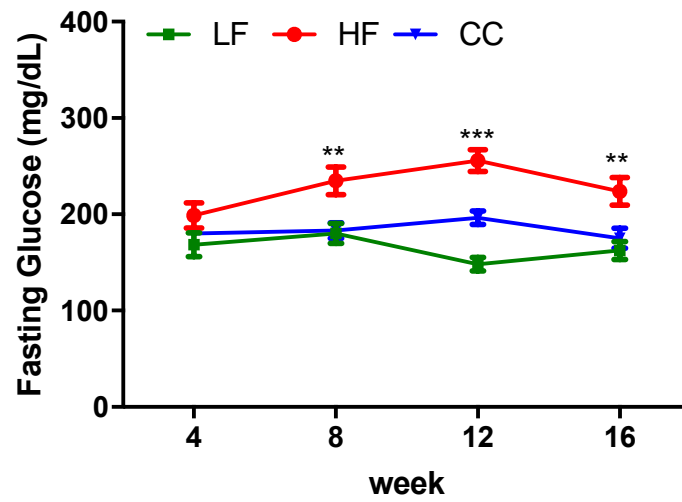


Figure 2. Average fasting blood glucose tested every 4-week period

Values are means \pm SEM, $n = 12$. * $P < 0.05$, ** $P < 0.01$, *** $P < 0.001$, and **** $P < 0.0001$ indicating significant difference between the HF and CC groups for every 4 weeks.

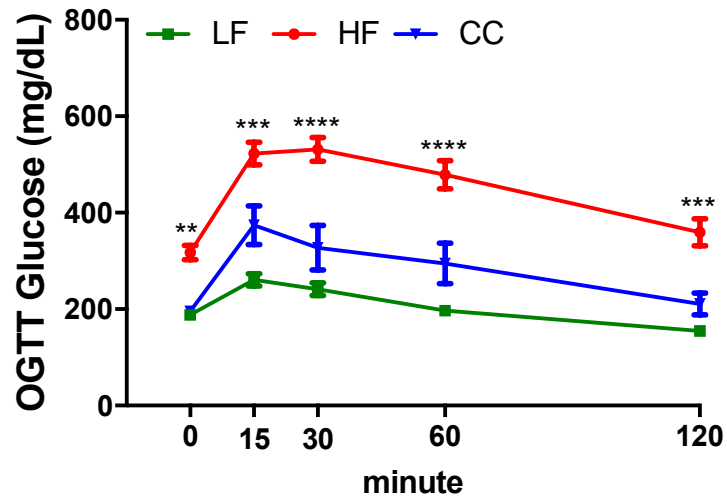


Figure 3. Average blood glucose measurement for oral glucose tolerance test over a 120-min period

Values are means \pm SEM, $n = 12$. * $P < 0.05$, ** $P < 0.01$, *** $P < 0.001$, and **** $P < 0.0001$ indicating significant difference between the HF and CC groups for every time point.

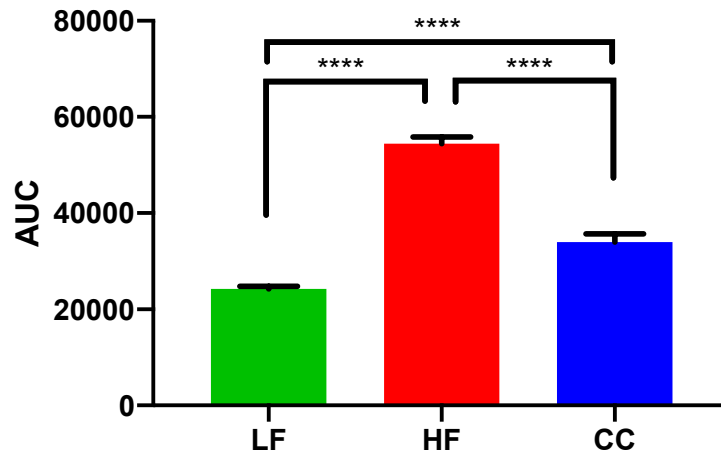


Figure 4. Average AUC calculated from OGTT levels from Figure 3

The baseline was set from 0. Values are means \pm SEM, $n = 12$, and * $P < 0.05$, ** $P < 0.01$, *** $P < 0.001$, and **** $P < 0.0001$ indicating significant difference among the LF, HF and CC groups.

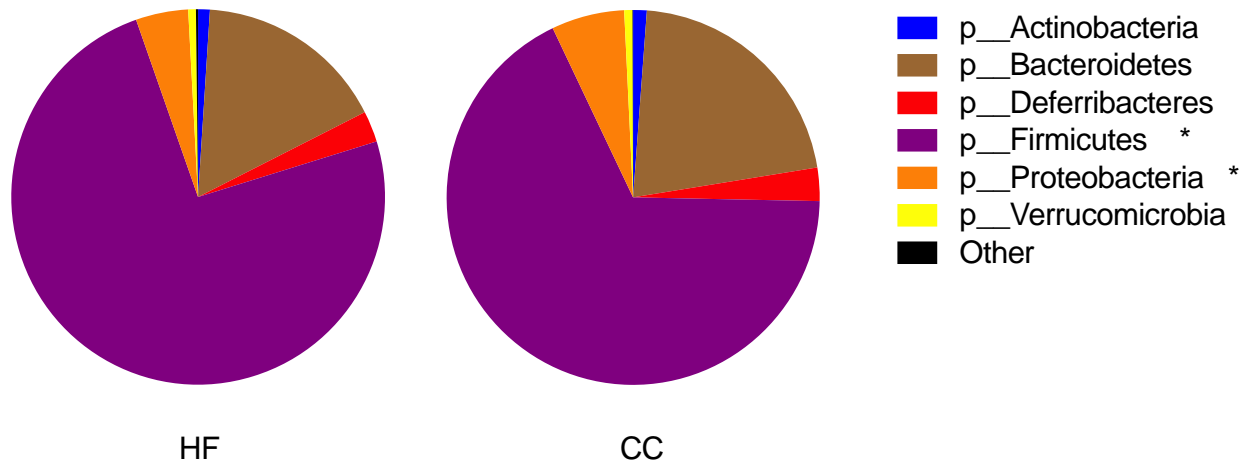


Figure 5. Relative abundance of microbiota at Phylum level between the HF and CC groups

Both the phyla of Firmicutes and Proteobacteria showed significantly elevated in the CC group compared to the HF group ($P < 0.05$), $n = 10$. Significance was indicated with * for $P < 0.05$, ** for $P < 0.01$, *** for $P < 0.001$, and **** for $P < 0.0001$.

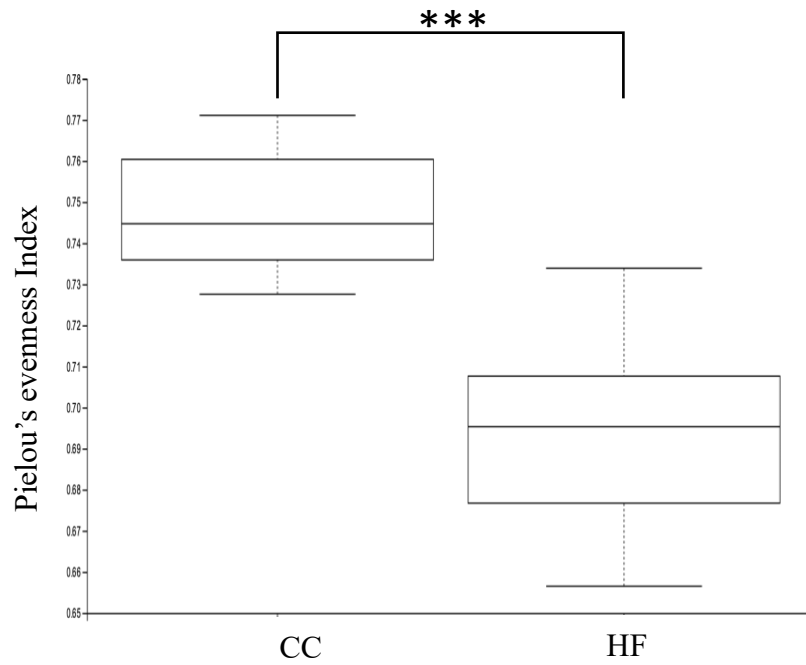


Figure 6. Pielou's evenness in alpha diversity between the HF and CC groups

Statistical analysis was performed using the Kruskal-Wallis test, $n = 10$ per group. Significance was indicated with * for $P < 0.05$, ** for $P < 0.01$, *** for $P < 0.001$, and **** for $P < 0.0001$.

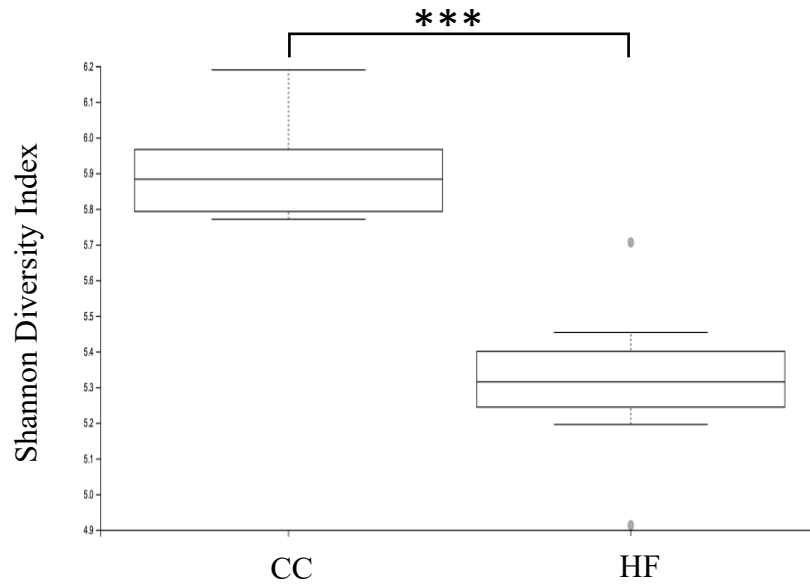


Figure 7. Shannon diversity index in alpha diversity between the HF and CC groups
Statistical analysis was performed using the Kruskal-Wallis test, $n = 10$ per group. Significance was indicated with * for $P < 0.05$, ** for $P < 0.01$, *** for $P < 0.001$, and **** for $P < 0.0001$.

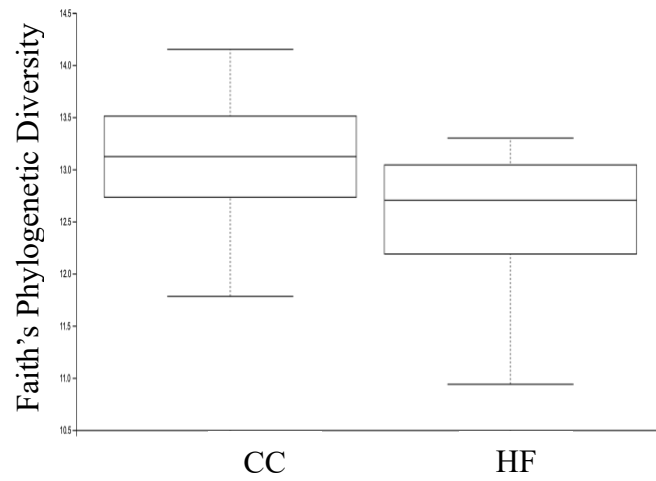


Figure 8. Faith's phylogenetic diversity (PD) in alpha diversity between the HF and CC groups

Statistical analysis was performed using the Kruskal-Wallis test, $n = 10$. $P = 0.13$. Significance was indicated with * for $P < 0.05$, ** for $P < 0.01$, *** for $P < 0.001$, and **** for $P < 0.0001$.

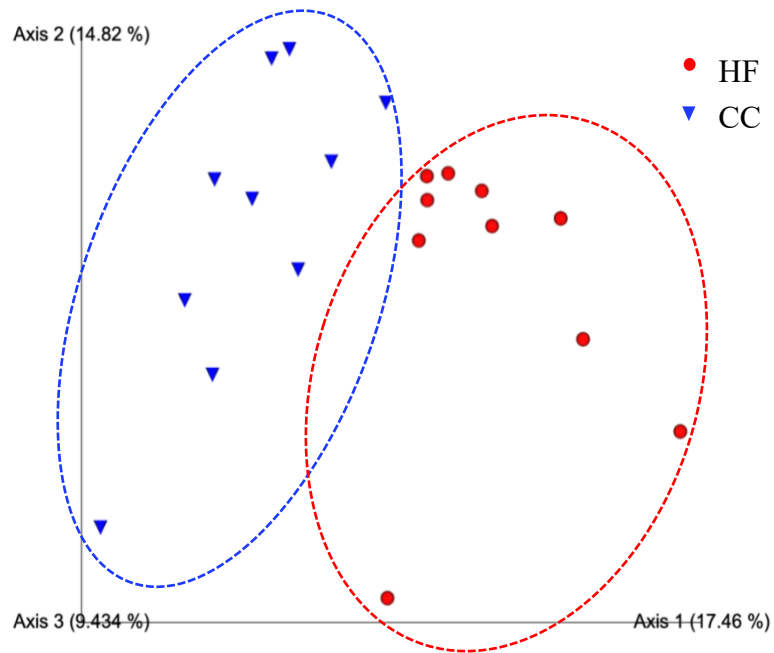


Figure 9. Unweighted Unifrac PCoA in beta diversity between the HF and CC groups
Statistical analysis was performed using the PERMANOVA, $P = 0.001$, $n = 10$ per group.

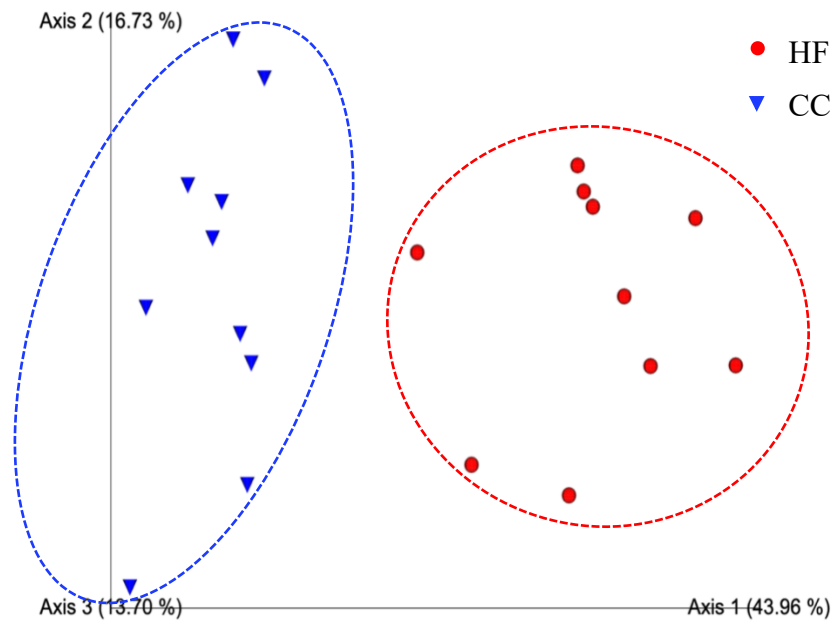


Figure 10. Weighted Unifrac PCoA in beta diversity between the HF and CC groups
Statistical analysis was performed using the PERMANOVA, $P = 0.001$, $n = 10$ per group.

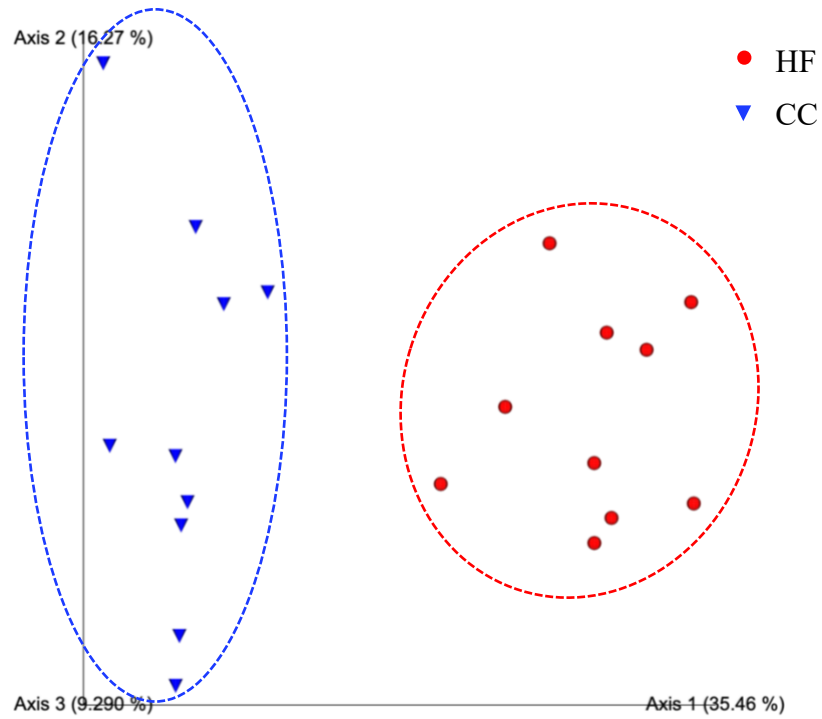


Figure 11. Bray-Curtis PCoA in beta diversity between the HF and CC groups
 Statistical analysis was performed using the PERMANOVA, $P = 0.001$, $n = 10$ per group.

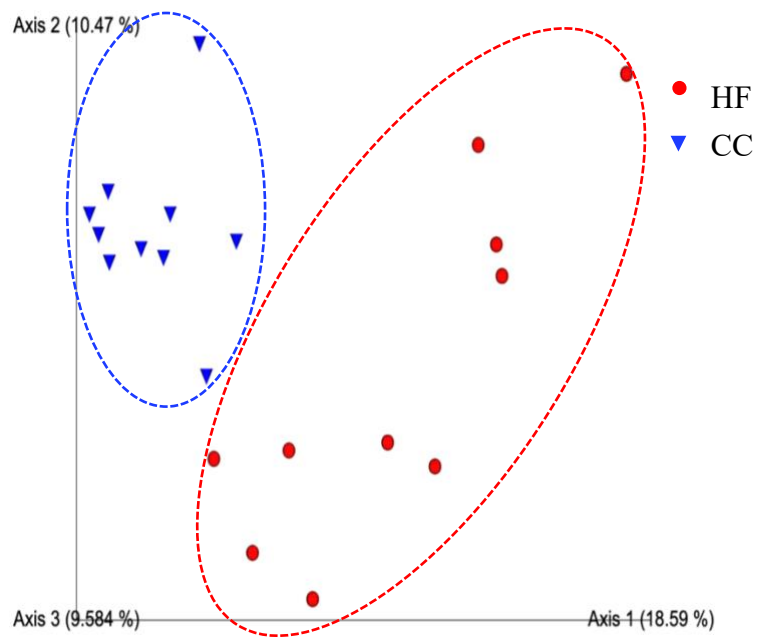


Figure 12. Jaccard PCoA in beta diversity between the HF and CC groups
Statistical analysis was performed using the PERMANOVA, $P = 0.001$, $n = 10$ per group.

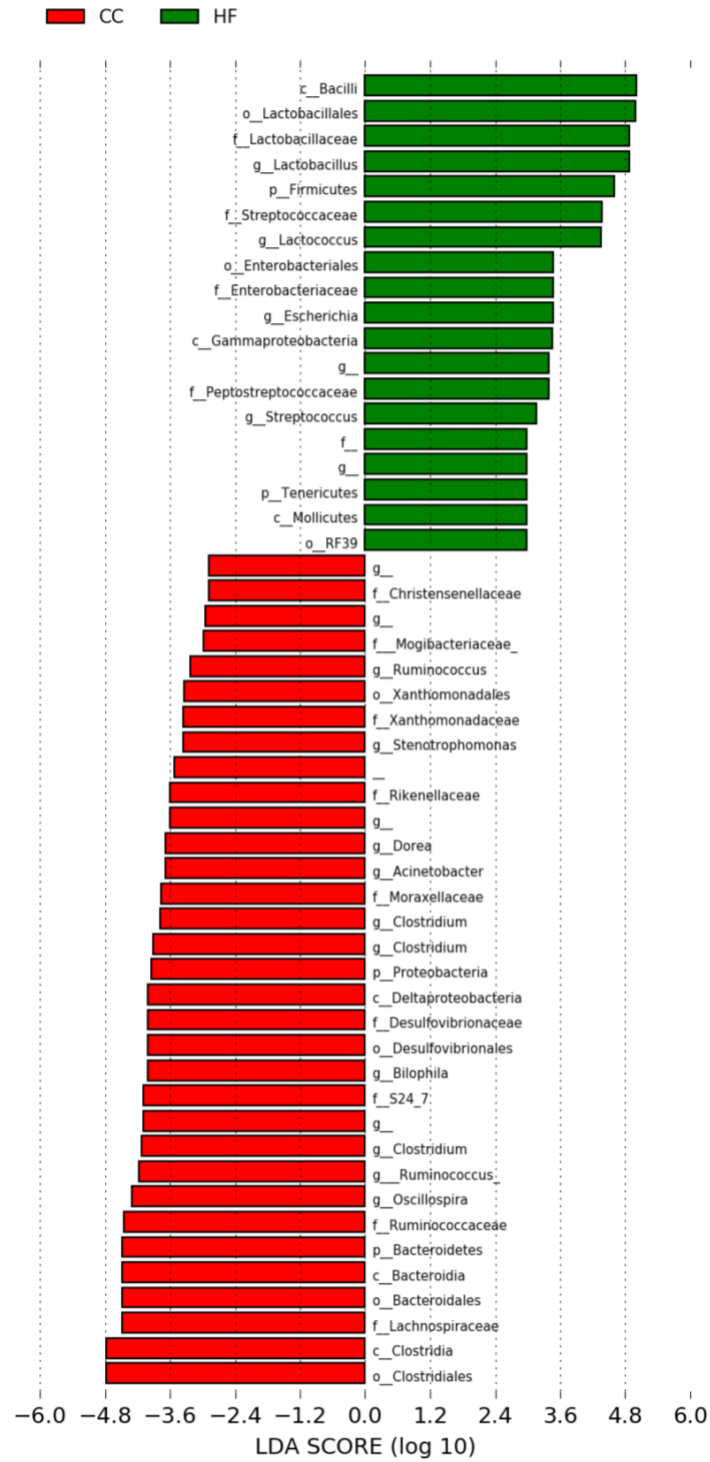


Figure 13. Biomarkers found by LEfSe results between the HF and CC groups

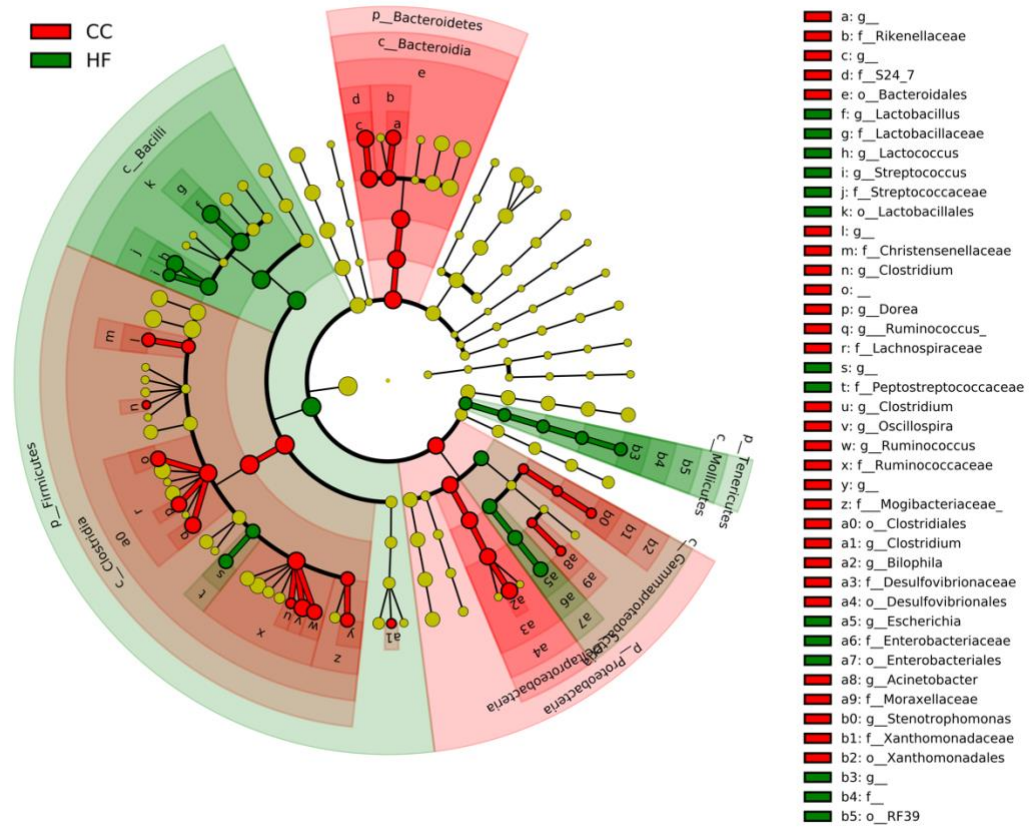


Figure 14. Cladograms of LEfSe results between the HF and CC groups

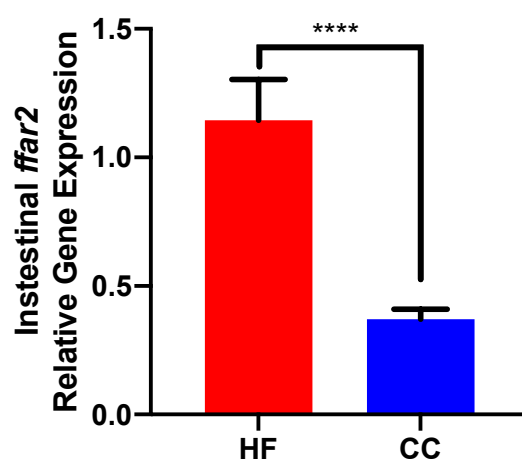


Figure 15. Intestinal *ffar2* relative gene expression

Values are means \pm SEM, n = 11-12, and *P < 0.05, **P < 0.01, ***P < 0.001, and ****P < 0.0001 indicating significant difference between the HF and CC groups.

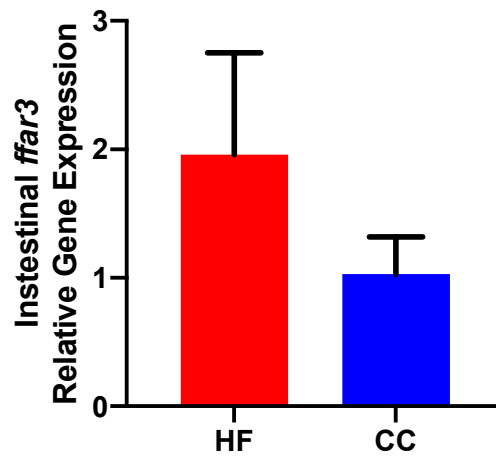


Figure 16. Intestinal *ffar3* relative gene expression

Values are means \pm SEM, n = 11-12, and *P < 0.05, **P < 0.01, ***P < 0.001, and ****P < 0.0001 indicating significant difference between the HF and CC groups.

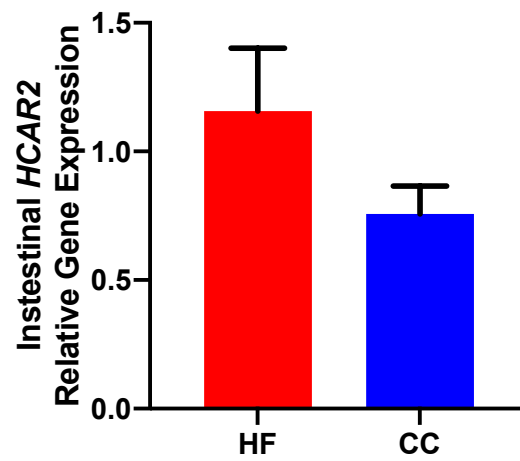


Figure 17. Intestinal *HCAR2* relative gene expression

Values are means \pm SEM, $n = 11-12$, and * $P < 0.05$, ** $P < 0.01$, *** $P < 0.001$, and **** $P < 0.0001$ indicating significant difference between the HF and CC groups.

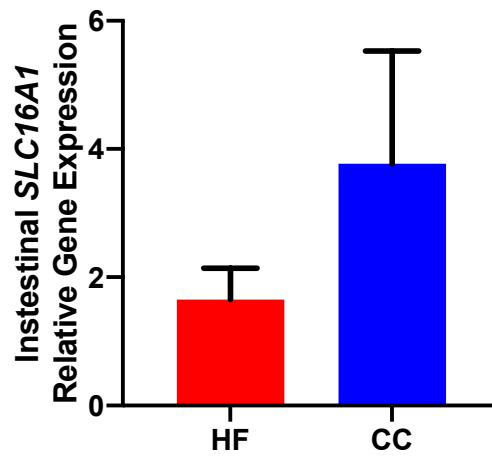


Figure 18. Intestinal *SLC16A1* relative gene expression

Values are means \pm SEM, n = 11-12, and *P < 0.05, **P < 0.01, ***P < 0.001, and ****P < 0.0001 indicating significant difference between the HF and CC groups.

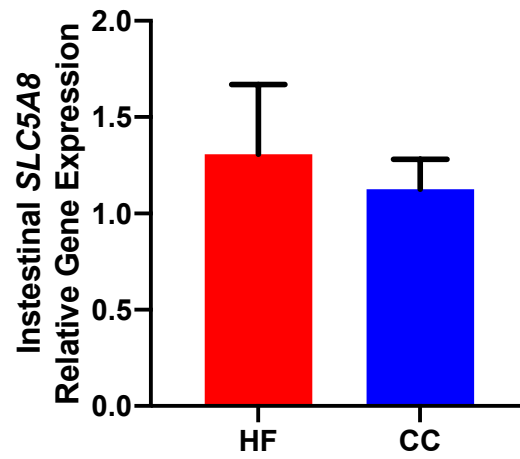


Figure 19. Intestinal *SLC5A8* relative gene expression

Values are means \pm SEM, $n = 11-12$, and * $P < 0.05$, ** $P < 0.01$, *** $P < 0.001$, and **** $P < 0.0001$ indicating significant difference between the HF and CC groups.

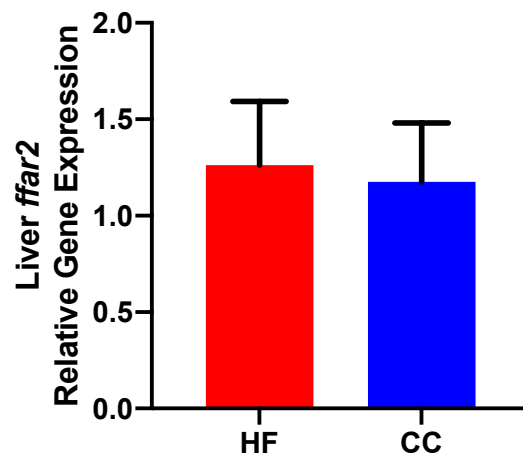


Figure 20. Liver *ffar2* relative gene expression

Values are means \pm SEM, $n = 11-12$, and * $P < 0.05$, ** $P < 0.01$, *** $P < 0.001$, and **** $P < 0.0001$ indicating significant difference between the HF and CC groups.

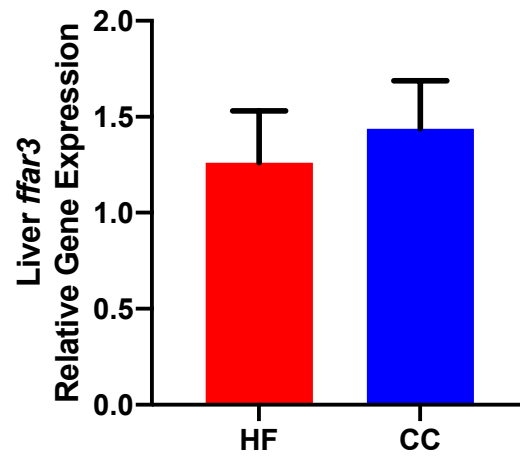


Figure 21. Liver *ffar3* relative gene expression

Values are means \pm SEM, n = 11-12, and *P < 0.05, **P < 0.01, ***P < 0.001, and ****P < 0.0001 indicating significant difference between the HF and CC groups.

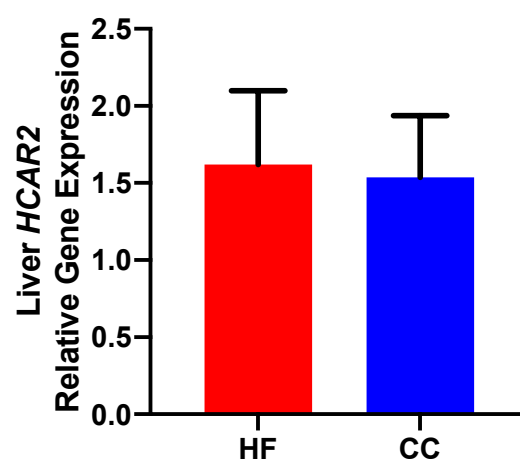


Figure 22. Liver *HCAR2* relative gene expression

Values are means \pm SEM, n = 11-12, and *P < 0.05, **P < 0.01, ***P < 0.001, and ****P < 0.0001 indicating significant difference between the HF and CC groups.

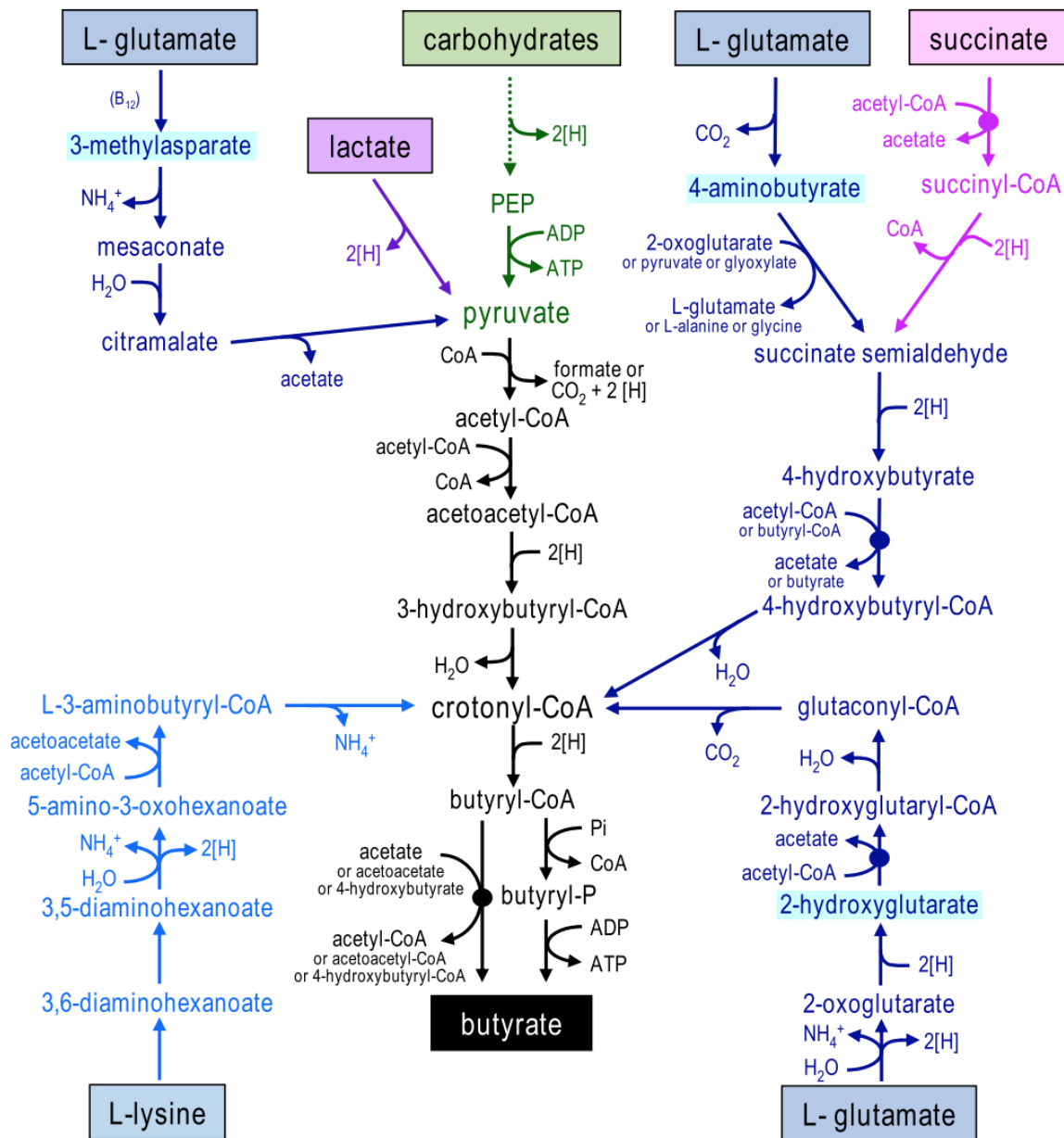


Figure 23. Butyrate synthesis pathways [160]

CoA, coenzyme A; P, bound phosphate; Pi, inorganic phosphate; PEP, phosphoenolpyruvate; (B₁₂), enzyme dependent on vitamin B₁₂. The dotted line indicates that several intermediate steps are involved.

REFERENCES

1. WHO. *Obesity and overweight*. 2020 [cited 2021 April 3]; Available from: <https://www.who.int/news-room/fact-sheets/detail/obesity-and-overweight>.
2. Hales, C.M., et al., *Prevalence of Obesity and Severe Obesity Among Adults: United States, 2017–2018*. NCHS Data Brief, 2020. **360**.
3. Hurley, M.M. and T.H. Moran, *Animal Models of Ingestive Behaviors*, in *Reference Module in Neuroscience and Biobehavioral Psychology*. 2020, Elsevier.
4. Hariri, N. and L. Thibault, *High-fat diet-induced obesity in animal models*. Nutr Res Rev, 2010. **23**(2): p. 270-99.
5. Service, U.S.D.o.A.A.R., *Nutrient intakes from food and beverages: mean amounts consumed per individual, by gender and age, what we eat in America, National Health and Nutrition Examination Survey 2015–2016*. 2018.
6. Gadde, K.M., et al., *Obesity: Pathophysiology and Management*. J Am Coll Cardiol, 2018. **71**(1): p. 69-84.
7. Chobot, A., et al., *Obesity and diabetes-Not only a simple link between two epidemics*. Diabetes Metab Res Rev, 2018. **34**(7): p. e3042.
8. Malone, J.I. and B.C. Hansen, *Does obesity cause type 2 diabetes mellitus (T2DM)? Or is it the opposite?* Pediatr Diabetes, 2019. **20**(1): p. 5-9.
9. Nguyen, N.T., et al., *Relationship between obesity and diabetes in a US adult population: findings from the National Health and Nutrition Examination Survey, 1999-2006*. Obes Surg, 2011. **21**(3): p. 351-5.
10. Daousi, C., et al., *Prevalence of obesity in type 2 diabetes in secondary care: association with cardiovascular risk factors*. Postgrad Med J, 2006. **82**(966): p. 280-4.

11. Landsberg, L., et al., *Obesity-related hypertension: pathogenesis, cardiovascular risk, and treatment: a position paper of The Obesity Society and the American Society of Hypertension*. J Clin Hypertens (Greenwich), 2013. **15**(1): p. 14-33.
12. Kotchen, T.A., *Obesity-related hypertension: epidemiology, pathophysiology, and clinical management*. Am J Hypertens, 2010. **23**(11): p. 1170-8.
13. Mittendorfer, B. and L.R. Peterson, *Cardiovascular Consequences of Obesity and Targets for Treatment*. Drug Discov Today Ther Strateg, 2008. **5**(1): p. 53-61.
14. Fontaine, K.R., et al., *Years of life lost due to obesity*. Jama, 2003. **289**(2): p. 187-93.
15. Chang, S.-H., L.M. Pollack, and G.A. Colditz, *Life Years Lost Associated with Obesity-Related Diseases for U.S. Non-Smoking Adults*. PloS one, 2013. **8**(6): p. e66550-e66550.
16. Hill, J.O., *Understanding and addressing the epidemic of obesity: an energy balance perspective*. Endocr Rev, 2006. **27**(7): p. 750-61.
17. Andela, S., et al., *Efficacy of very low-energy diet programs for weight loss: A systematic review with meta-analysis of intervention studies in children and adolescents with obesity*. Obes Rev, 2019. **20**(6): p. 871-882.
18. Kim, B.Y., et al., *Obesity and Physical Activity*. J Obes Metab Syndr, 2017. **26**(1): p. 15-22.
19. Thorogood, A., et al., *Isolated aerobic exercise and weight loss: a systematic review and meta-analysis of randomized controlled trials*. Am J Med, 2011. **124**(8): p. 747-55.
20. Fock, K.M. and J. Khoo, *Diet and exercise in management of obesity and overweight*. J Gastroenterol Hepatol, 2013. **28 Suppl 4**: p. 59-63.

21. Johns, D.J., et al., *Diet or exercise interventions vs combined behavioral weight management programs: a systematic review and meta-analysis of direct comparisons*. J Acad Nutr Diet, 2014. **114**(10): p. 1557-68.
22. Sekirov, I., et al., *Gut microbiota in health and disease*. Physiol Rev, 2010. **90**(3): p. 859-904.
23. Zhang, Y.J., et al., *Impacts of gut bacteria on human health and diseases*. Int J Mol Sci, 2015. **16**(4): p. 7493-519.
24. Gérard, P., *Gut microbiota and obesity*. Cellular and Molecular Life Sciences, 2016. **73**(1): p. 147-162.
25. Clemente, J.C., et al., *The impact of the gut microbiota on human health: an integrative view*. Cell, 2012. **148**(6): p. 1258-70.
26. Singh, R.K., et al., *Influence of diet on the gut microbiome and implications for human health*. J Transl Med, 2017. **15**(1): p. 73.
27. Dethlefsen, L., et al., *The pervasive effects of an antibiotic on the human gut microbiota, as revealed by deep 16S rRNA sequencing*. PLoS Biol, 2008. **6**(11): p. e280.
28. Zhang, C., et al., *Interactions between gut microbiota, host genetics and diet relevant to development of metabolic syndromes in mice*. Isme j, 2010. **4**(2): p. 232-41.
29. Arumugam, M., et al., *Enterotypes of the human gut microbiome*. Nature, 2011. **473**(7346): p. 174-80.
30. Wu, G.D., et al., *Linking long-term dietary patterns with gut microbial enterotypes*. Science, 2011. **334**(6052): p. 105-8.
31. Karlsson, F., et al., *Assessing the human gut microbiota in metabolic diseases*. Diabetes, 2013. **62**(10): p. 3341-9.

32. Meldrum, D.R., M.A. Morris, and J.C. Gambone, *Obesity pandemic: causes, consequences, and solutions-but do we have the will?* Fertil Steril, 2017. **107**(4): p. 833-839.
33. John, G.K. and G.E. Mullin, *The Gut Microbiome and Obesity*. Curr Oncol Rep, 2016. **18**(7): p. 45.
34. Sweeney, T.E. and J.M. Morton, *The human gut microbiome: a review of the effect of obesity and surgically induced weight loss*. JAMA Surg, 2013. **148**(6): p. 563-9.
35. Koliada, A., et al., *Association between body mass index and Firmicutes/Bacteroidetes ratio in an adult Ukrainian population*. BMC Microbiol, 2017. **17**(1): p. 120.
36. Ley, R.E., et al., *Microbial ecology: human gut microbes associated with obesity*. Nature, 2006. **444**(7122): p. 1022-3.
37. Tilg, H., *Gut microbiome, obesity, and metabolic dysfunction*. 2011. **121**(6): p. 2126-32.
38. Turnbaugh, P.J., et al., *An obesity-associated gut microbiome with increased capacity for energy harvest*. Nature, 2006. **444**(7122): p. 1027-31.
39. Bäckhed, F., et al., *Mechanisms underlying the resistance to diet-induced obesity in germ-free mice*. Proc Natl Acad Sci U S A, 2007. **104**(3): p. 979-84.
40. Backhed, F., et al., *The gut microbiota as an environmental factor that regulates fat storage*. Proc Natl Acad Sci U S A, 2004. **101**(44): p. 15718-23.
41. Brown, J.M. and S.L. Hazen, *Microbial modulation of cardiovascular disease*. Nat Rev Microbiol, 2018.
42. Udayappan, S., et al., *Oral treatment with Eubacterium hallii improves insulin sensitivity in db/db mice*. npj Biofilms and Microbiomes, 2016. **2**: p. 16009.
43. Trajkovski, M. and C.B. Wollheim, *Physiology: Microbial signals to the brain control weight*. Nature, 2016. **534**(7606): p. 185-187.

44. Bermudez-Brito, M., et al., *Probiotic mechanisms of action*. Ann Nutr Metab, 2012. **61**(2): p. 160-74.
45. Hemarajata, P. and J. Versalovic, *Effects of probiotics on gut microbiota: mechanisms of intestinal immunomodulation and neuromodulation*. Therap Adv Gastroenterol, 2013. **6**(1): p. 39-51.
46. Yan, F. and D. Polk, *Probiotics and immune health*. Current opinion in gastroenterology, 2011. **27**(6): p. 496.
47. Singh, V.P., et al., *Role of probiotics in health and disease: a review*. J Pak Med Assoc, 2013. **63**(2): p. 253-7.
48. O'Shea, E.F., et al., *Production of bioactive substances by intestinal bacteria as a basis for explaining probiotic mechanisms: bacteriocins and conjugated linoleic acid*. Int J Food Microbiol, 2012. **152**(3): p. 189-205.
49. Collado, M.C., J. Meriluoto, and S. Salminen, *Role of commercial probiotic strains against human pathogen adhesion to intestinal mucus*. Lett Appl Microbiol, 2007. **45**(4): p. 454-60.
50. Neeser, J.R., et al., *Lactobacillus johnsonii La1 shares carbohydrate-binding specificities with several enteropathogenic bacteria*. Glycobiology, 2000. **10**(11): p. 1193-9.
51. Mathipa, M.G. and M.S. Thantsha, *Probiotic engineering: towards development of robust probiotic strains with enhanced functional properties and for targeted control of enteric pathogens*. Gut Pathog, 2017. **9**: p. 28.
52. Vilà, B., E. Esteve-Garcia, and J. Brufau, *Probiotic micro-organisms: 100 years of innovation and efficacy; modes of action*. World's Poultry Science Journal, 2010. **66**(3): p. 369-380.

53. Plaza-Diaz, J., et al., *Mechanisms of Action of Probiotics*. Adv Nutr, 2019. **10**(suppl_1): p. S49-s66.
54. Kobyliak, N., et al., *Probiotics in prevention and treatment of obesity: a critical view*. Nutr Metab (Lond), 2016. **13**: p. 14.
55. Morrison, D.J. and T. Preston, *Formation of short chain fatty acids by the gut microbiota and their impact on human metabolism*. Gut Microbes, 2016. **7**(3): p. 189-200.
56. Butel, M.J., *Probiotics, gut microbiota and health*. Med Mal Infect, 2014. **44**(1): p. 1-8.
57. Yan, F. and D.B. Polk, *Probiotics: progress toward novel therapies for intestinal diseases*. Curr Opin Gastroenterol, 2010. **26**(2): p. 95-101.
58. Lu, Y., et al., *Short Chain Fatty Acids Prevent High-fat-diet-induced Obesity in Mice by Regulating G Protein-coupled Receptors and Gut Microbiota*. Scientific Reports, 2016. **6**(1): p. 37589.
59. Tolhurst, G., et al., *Short-chain fatty acids stimulate glucagon-like peptide-1 secretion via the G-protein-coupled receptor FFAR2*. Diabetes, 2012. **61**(2): p. 364-71.
60. Samuel, B.S., et al., *Effects of the gut microbiota on host adiposity are modulated by the short-chain fatty-acid binding G protein-coupled receptor, Gpr41*. Proc Natl Acad Sci U S A, 2008. **105**(43): p. 16767-72.
61. Liu, H., et al., *Butyrate: A Double-Edged Sword for Health?* Adv Nutr, 2018. **9**(1): p. 21-29.
62. Chakraborti, C.K., *New-found link between microbiota and obesity*. World journal of gastrointestinal pathophysiology, 2015. **6**(4): p. 110.

63. Den Besten, G., et al., *The role of short-chain fatty acids in the interplay between diet, gut microbiota, and host energy metabolism*. Journal of Lipid Research, 2013. **54**(9): p. 2325-2340.
64. Lee, W.K., et al., *Isolation and identification of clostridia from the intestine of laboratory animals*. Lab Anim, 1991. **25**(1): p. 9-15.
65. Finegold, S.M., et al., *Gastrointestinal microflora studies in late-onset autism*. Clin Infect Dis, 2002. **35**(Suppl 1): p. S6-S16.
66. Yutin, N. and M.Y. Galperin, *A genomic update on clostridial phylogeny: Gram-negative spore formers and other misplaced clostridia*. Environ Microbiol, 2013. **15**(10): p. 2631-41.
67. Sanchez Ramos, L. and A.C. Rodloff, *Identification of Clostridium species using the VITEK(®) MS*. Anaerobe, 2018. **54**: p. 217-223.
68. Gibbs, P.A., *23 - Pathogenic Clostridium species*, in *Foodborne Pathogens (Second Edition)*, C.d.W. Blackburn and P.J. McClure, Editors. 2009, Woodhead Publishing. p. 820-843.
69. Cassir, N., S. Benamar, and B. La Scola, *Clostridium butyricum: from beneficial to a new emerging pathogen*. Clin Microbiol Infect, 2016. **22**(1): p. 37-45.
70. Shang, H., J. Sun, and Y.Q. Chen, *Clostridium Butyricum CGMCC0313.1 Modulates Lipid Profile, Insulin Resistance and Colon Homeostasis in Obese Mice*. PLoS One, 2016. **11**(4): p. e0154373.
71. Jia, L., et al., *Anti-diabetic Effects of Clostridium butyricum CGMCC0313.1 through Promoting the Growth of Gut Butyrate-producing Bacteria in Type 2 Diabetic Mice*. Sci Rep, 2017. **7**(1): p. 7046.

72. Buckel, W. and H.A. Barker, *Two pathways of glutamate fermentation by anaerobic bacteria*. J Bacteriol, 1974. **117**(3): p. 1248-60.
73. Leutbecher, U., et al., *Glutamate mutase from Clostridium cochlearium. Purification, cobamide content and stereospecific inhibitors*. Eur J Biochem, 1992. **205**(2): p. 759-65.
74. Gao, Z., et al., *Butyrate improves insulin sensitivity and increases energy expenditure in mice*. Diabetes, 2009. **58**(7): p. 1509-17.
75. Udayappan, S., et al., *Oral treatment with Eubacterium hallii improves insulin sensitivity in db/db mice*. NPJ Biofilms Microbiomes, 2016. **2**: p. 16009.
76. Duncan, S.H., P. Louis, and H.J. Flint, *Lactate-utilizing bacteria, isolated from human feces, that produce butyrate as a major fermentation product*. Appl Environ Microbiol, 2004. **70**(10): p. 5810-7.
77. Zhou, A.L., et al., *Whole grain oats improve insulin sensitivity and plasma cholesterol profile and modify gut microbiota composition in C57BL/6J mice*. J Nutr, 2015. **145**(2): p. 222-30.
78. Murakami, N., et al., *Mice heterozygous for the xanthine oxidoreductase gene facilitate lipid accumulation in adipocytes*. Arterioscler Thromb Vasc Biol, 2014. **34**(1): p. 44-51.
79. Hu, C.C., K. Qing, and Y. Chen, *Diet-induced changes in stearyl-CoA desaturase 1 expression in obesity-prone and -resistant mice*. Obes Res, 2004. **12**(8): p. 1264-70.
80. Siersbæk, M.S., et al., *C57BL/6J substrain differences in response to high-fat diet intervention*. Sci Rep, 2020. **10**(1): p. 14052.
81. Kuriyan, R., *Body composition techniques*. Indian J Med Res, 2018. **148**(5): p. 648-658.

82. Marvyn, P.M., et al., *Data on oxygen consumption rate, respiratory exchange ratio, and movement in C57BL/6J female mice on the third day of consuming a high-fat diet*. Data Brief, 2016. **7**: p. 472-5.
83. Hoffmans, M., et al., *Resting metabolic rate in obese and normal weight women*. Int J Obes, 1979. **3**(2): p. 111-8.
84. Amaro-Gahete, F.J., et al., *Association of basal metabolic rate and fuel oxidation in basal conditions and during exercise, with plasma S-klotho: the FIT-AGEING study*. Aging (Albany NY), 2019. **11**(15): p. 5319-5333.
85. Achten, J. and A.E. Jeukendrup, *Optimizing fat oxidation through exercise and diet*. Nutrition, 2004. **20**(7-8): p. 716-27.
86. Sukkar, A.H., et al., *Regulation of energy expenditure and substrate oxidation by short-chain fatty acids*. J Endocrinol, 2019. **242**(2): p. R1-R8.
87. Ursell, L.K., et al., *Defining the human microbiome*. Nutr Rev, 2012. **70 Suppl 1**(Suppl 1): p. S38-44.
88. Davidson, R.M. and L.E. Epperson, *Microbiome Sequencing Methods for Studying Human Diseases*. Methods Mol Biol, 2018. **1706**: p. 77-90.
89. Clarridge, J.E., 3rd, *Impact of 16S rRNA gene sequence analysis for identification of bacteria on clinical microbiology and infectious diseases*. Clin Microbiol Rev, 2004. **17**(4): p. 840-62, table of contents.
90. Johnson, J.S., et al., *Evaluation of 16S rRNA gene sequencing for species and strain-level microbiome analysis*. Nature Communications, 2019. **10**(1): p. 5029.

91. Kozich, J.J., et al., *Development of a dual-index sequencing strategy and curation pipeline for analyzing amplicon sequence data on the MiSeq Illumina sequencing platform*. Appl Environ Microbiol, 2013. **79**(17): p. 5112-20.
92. Bolyen, E., et al., *Reproducible, interactive, scalable and extensible microbiome data science using QIIME 2*. Nat Biotechnol, 2019. **37**(8): p. 852-857.
93. Callahan, B.J., et al., *DADA2: High-resolution sample inference from Illumina amplicon data*. Nat Methods, 2016. **13**(7): p. 581-3.
94. Lawley, B. and G.W. Tannock, *Analysis of 16S rRNA gene amplicon sequences using the QIIME software package*, in *Oral Biology*. 2017, Springer. p. 153-163.
95. Lopez-Garcia, A., et al., *Comparison of Mothur and QIIME for the Analysis of Rumen Microbiota Composition Based on 16S rRNA Amplicon Sequences*. Front Microbiol, 2018. **9**: p. 3010.
96. Bokulich, N.A., et al., *q2-longitudinal: Longitudinal and Paired-Sample Analyses of Microbiome Data*. mSystems, 2018. **3**(6).
97. Segata, N., et al., *Metagenomic biomarker discovery and explanation*. Genome Biol, 2011. **12**(6): p. R60.
98. Moreira, G., et al., *Liraglutide modulates gut microbiota and reduces NAFLD in obese mice*. The Journal of nutritional biochemistry, 2018. **62**: p. 143-154.
99. Koh, H., *An adaptive microbiome α -diversity-based association analysis method*. Sci Rep, 2018. **8**(1): p. 18026.
100. Gail, M.H., Y. Wan, and J. Shi, *Power of Microbiome Beta-Diversity Analyses Based on Standard Reference Samples*. Am J Epidemiol, 2021. **190**(3): p. 439-447.

101. Dahiya, D.K., et al., *Gut Microbiota Modulation and Its Relationship with Obesity Using Prebiotic Fibers and Probiotics: A Review*. Front Microbiol, 2017. **8**: p. 563.
102. Reese, A.T. and R.R. Dunn, *Drivers of Microbiome Biodiversity: A Review of General Rules, Feces, and Ignorance*. mBio, 2018. **9**(4).
103. Chakraborti, C.K., *New-found link between microbiota and obesity*. World J Gastrointest Pathophysiol, 2015. **6**(4): p. 110-9.
104. Turnbaugh, P.J., et al., *A core gut microbiome in obese and lean twins*. Nature, 2009. **457**(7228): p. 480-4.
105. Le Chatelier, E., et al., *Richness of human gut microbiome correlates with metabolic markers*. Nature, 2013. **500**: p. 541.
106. Claesson, M.J., et al., *Gut microbiota composition correlates with diet and health in the elderly*. Nature, 2012. **488**(7410): p. 178-84.
107. Lepage, P., et al., *Twin study indicates loss of interaction between microbiota and mucosa of patients with ulcerative colitis*. Gastroenterology, 2011. **141**(1): p. 227-36.
108. Manichanh, C., et al., *Reduced diversity of faecal microbiota in Crohn's disease revealed by a metagenomic approach*. Gut, 2006. **55**(2): p. 205-11.
109. Goodrich, J.K., et al., *Conducting a microbiome study*. Cell, 2014. **158**(2): p. 250-262.
110. Chung, N.C., et al., *Jaccard/Tanimoto similarity test and estimation methods for biological presence-absence data*. BMC Bioinformatics, 2019. **20**(Suppl 15): p. 644.
111. Magne, F., et al., *The Firmicutes/Bacteroidetes Ratio: A Relevant Marker of Gut Dysbiosis in Obese Patients?* Nutrients, 2020. **12**(5).
112. Tseng, C.H. and C.Y. Wu, *The gut microbiome in obesity*. J Formos Med Assoc, 2019. **118** Suppl 1: p. S3-s9.

113. Castaner, O., et al., *The Gut Microbiome Profile in Obesity: A Systematic Review*. Int J Endocrinol, 2018. **2018**: p. 4095789.
114. Ley, R.E., et al., *Obesity alters gut microbial ecology*. Proc Natl Acad Sci U S A, 2005. **102**(31): p. 11070-5.
115. Turnbaugh, P.J., et al., *Diet-induced obesity is linked to marked but reversible alterations in the mouse distal gut microbiome*. Cell Host Microbe, 2008. **3**(4): p. 213-23.
116. Krajmalnik-Brown, R., et al., *Effects of gut microbes on nutrient absorption and energy regulation*. Nutr Clin Pract, 2012. **27**(2): p. 201-14.
117. Shin, N.R., T.W. Whon, and J.W. Bae, *Proteobacteria: microbial signature of dysbiosis in gut microbiota*. Trends Biotechnol, 2015. **33**(9): p. 496-503.
118. Wang, J., et al., *Modulation of gut microbiota during probiotic-mediated attenuation of metabolic syndrome in high fat diet-fed mice*. ISME J, 2015. **9**(1): p. 1-15.
119. Everard, A., et al., *Responses of gut microbiota and glucose and lipid metabolism to prebiotics in genetic obese and diet-induced leptin-resistant mice*. Diabetes, 2011. **60**(11): p. 2775-86.
120. Zhu, L., et al., *Characterization of gut microbiomes in nonalcoholic steatohepatitis (NASH) patients: a connection between endogenous alcohol and NASH*. Hepatology, 2013. **57**(2): p. 601-9.
121. Esquivel-Elizondo, S., et al., *Insights into Butyrate Production in a Controlled Fermentation System via Gene Predictions*. mSystems, 2017. **2**(4).
122. Peters, B.A., et al., *A taxonomic signature of obesity in a large study of American adults*. Sci Rep, 2018. **8**(1): p. 9749.

123. de la Cuesta-Zuluaga, J., et al., *Gut microbiota is associated with obesity and cardiometabolic disease in a population in the midst of Westernization*. Sci Rep, 2018. **8**(1): p. 11356.
124. Truax, A.D., et al., *The Inhibitory Innate Immune Sensor NLRP12 Maintains a Threshold against Obesity by Regulating Gut Microbiota Homeostasis*. Cell Host Microbe, 2018. **24**(3): p. 364-378.e6.
125. Flemer, B., et al., *The oral microbiota in colorectal cancer is distinctive and predictive*. Gut, 2018. **67**(8): p. 1454-1463.
126. Rai, R., V.A. Saraswat, and R.K. Dhiman, *Gut microbiota: its role in hepatic encephalopathy*. Journal of clinical and experimental hepatology, 2015. **5**(Suppl 1): p. S29-S36.
127. Guo, S., et al., *Anti-Obesity and Gut Microbiota Modulation Effect of Secoiridoid-Enriched Extract from Fraxinus mandshurica Seeds on High-Fat Diet-Fed Mice*. Molecules, 2020. **25**(17).
128. Karvonen, A.M., et al., *Gut microbiota and overweight in 3-year old children*. Int J Obes (Lond), 2019. **43**(4): p. 713-723.
129. Ottosson, F., et al., *Connection Between BMI-Related Plasma Metabolite Profile and Gut Microbiota*. The Journal of Clinical Endocrinology & Metabolism, 2018. **103**(4): p. 1491-1501.
130. Oki, K., et al., *Comprehensive analysis of the fecal microbiota of healthy Japanese adults reveals a new bacterial lineage associated with a phenotype characterized by a high frequency of bowel movements and a lean body type*. BMC Microbiology, 2016. **16**(1): p. 284.

131. Calderón-Pérez, L., et al., *Gut metagenomic and short chain fatty acids signature in hypertension: a cross-sectional study*. Scientific Reports, 2020. **10**(1): p. 6436.
132. Goodrich, J.K., et al., *Human genetics shape the gut microbiome*. Cell, 2014. **159**(4): p. 789-99.
133. Waters, J.L. and R.E. Ley, *The human gut bacteria Christensenellaceae are widespread, heritable, and associated with health*. BMC Biology, 2019. **17**(1): p. 83.
134. Nilsen, M., et al., *Butyrate Levels in the Transition from an Infant- to an Adult-Like Gut Microbiota Correlate with Bacterial Networks Associated with Eubacterium Rectale and Ruminococcus Gnavus*. Genes (Basel), 2020. **11**(11).
135. Liu, S., et al., *Altered gut microbiota and short chain fatty acids in Chinese children with autism spectrum disorder*. Scientific Reports, 2019. **9**(1): p. 287.
136. Garber, A., P. Hastie, and J.-A. Murray, *Factors Influencing Equine Gut Microbiota: Current Knowledge*. Journal of Equine Veterinary Science, 2020. **88**: p. 102943.
137. Rouxinol-Dias, A.L., et al., *Probiotics for the control of obesity - Its effect on weight change*. Porto Biomed J, 2016. **1**(1): p. 12-24.
138. Raoult, D., *Probiotics and obesity: a link?* Nature Reviews Microbiology, 2009. **7**(9): p. 616-616.
139. Chang, Y.H., et al., *Selection of a potential probiotic Lactobacillus strain and subsequent in vivo studies*. Antonie Van Leeuwenhoek, 2001. **80**(2): p. 193-9.
140. Million, M., et al., *Obesity-associated gut microbiota is enriched in Lactobacillus reuteri and depleted in Bifidobacterium animalis and Methanobrevibacter smithii*. Int J Obes (Lond), 2012. **36**(6): p. 817-25.

141. Lu, Y.C., et al., *Effect of Lactobacillus reuteri GMNL-263 treatment on renal fibrosis in diabetic rats*. J Biosci Bioeng, 2010. **110**(6): p. 709-15.
142. Million, M., et al., *Comparative meta-analysis of the effect of Lactobacillus species on weight gain in humans and animals*. Microb Pathog, 2012. **53**(2): p. 100-8.
143. Kim, D., et al., *Lactococcus lactis BFE920 activates the innate immune system of olive flounder (Paralichthys olivaceus), resulting in protection against Streptococcus iniae infection and enhancing feed efficiency and weight gain in large-scale field studies*. Fish Shellfish Immunol, 2013. **35**(5): p. 1585-90.
144. Hadjisymeou, S., P. Loizou, and P. Kothari, *Lactococcus lactis cremoris infection: not rare anymore?* BMJ Case Rep, 2013. **2013**.
145. Balvočiūtė, M. and D.H. Huson, *SILVA, RDP, Greengenes, NCBI and OTT—how do these taxonomies compare?* BMC Genomics, 2017. **18**(2): p. 114.
146. Pope, L. and L.J. Rode, *Spore fine structure in Clostridium cochlearium*. J Bacteriol, 1969. **100**(2): p. 994-1001.
147. Korza, G., et al., *Changes in Bacillus Spore Small Molecules, rRNA, Germination, and Outgrowth after Extended Sublethal Exposure to Various Temperatures: Evidence that Protein Synthesis Is Not Essential for Spore Germination*. J Bacteriol, 2016. **198**(24): p. 3254-3264.
148. Douglas, G.M., et al., *PICRUSt2 for prediction of metagenome functions*. Nature Biotechnology, 2020. **38**(6): p. 685-688.
149. Sheflin, A.M., et al., *Dietary supplementation with rice bran or navy bean alters gut bacterial metabolism in colorectal cancer survivors*. Mol Nutr Food Res, 2017. **61**(1).

150. Bunyavanich, S., et al., *Early-life gut microbiome composition and milk allergy resolution*. J Allergy Clin Immunol, 2016. **138**(4): p. 1122-1130.
151. Garcia-Mazcorro, J.F., et al., *Comprehensive Molecular Characterization of Bacterial Communities in Feces of Pet Birds Using 16S Marker Sequencing*. Microb Ecol, 2017. **73**(1): p. 224-235.
152. Louca, S. and M. Doebeli, *Efficient comparative phylogenetics on large trees*. Bioinformatics, 2018. **34**(6): p. 1053-1055.
153. Ye, Y. and T.G. Doak, *A Parsimony Approach to Biological Pathway Reconstruction/Inference for Genomes and Metagenomes*. PLOS Computational Biology, 2009. **5**(8): p. e1000465.
154. Zheng, X., et al., *A targeted metabolomic protocol for short-chain fatty acids and branched-chain amino acids*. Metabolomics, 2013. **9**(4): p. 818-827.
155. Kaspar, H., *Amino acid analysis in biological fluids by GC-MS*. 2009.
156. Lefever, S., et al., *RDML: structured language and reporting guidelines for real-time quantitative PCR data*. Nucleic Acids Res, 2009. **37**(7): p. 2065-9.
157. Yuan, J.S., et al., *Statistical analysis of real-time PCR data*. BMC Bioinformatics, 2006. **7**: p. 85.
158. Parada Venegas, D., et al., *Short Chain Fatty Acids (SCFAs)-Mediated Gut Epithelial and Immune Regulation and Its Relevance for Inflammatory Bowel Diseases*. Front Immunol, 2019. **10**: p. 277.
159. den Besten, G., et al., *The role of short-chain fatty acids in the interplay between diet, gut microbiota, and host energy metabolism*. J Lipid Res, 2013. **54**(9): p. 2325-40.

160. Louis, P. and H.J. Flint, *Formation of propionate and butyrate by the human colonic microbiota*. Environ Microbiol, 2017. **19**(1): p. 29-41.
161. Millard, P., et al., *Control and regulation of acetate overflow in Escherichia coli*. Elife, 2021. **10**.
162. de la Cuesta-Zuluaga, J., et al., *Higher Fecal Short-Chain Fatty Acid Levels Are Associated with Gut Microbiome Dysbiosis, Obesity, Hypertension and Cardiometabolic Disease Risk Factors*. Nutrients, 2018. **11**(1).
163. Teixeira, T.F., et al., *Higher level of faecal SCFA in women correlates with metabolic syndrome risk factors*. Br J Nutr, 2013. **109**(5): p. 914-9.
164. Koh, A., et al., *From Dietary Fiber to Host Physiology: Short-Chain Fatty Acids as Key Bacterial Metabolites*. Cell, 2016. **165**(6): p. 1332-1345.
165. Wong, J.M.W. and D.J.A. Jenkins, *Carbohydrate Digestibility and Metabolic Effects*. The Journal of Nutrition, 2007. **137**(11): p. 2539S-2546S.
166. Natarajan, N., et al., *Microbial short chain fatty acid metabolites lower blood pressure via endothelial G protein-coupled receptor 41*. Physiol Genomics, 2016. **48**(11): p. 826-834.
167. Müller, M., et al., *Circulating but not faecal short-chain fatty acids are related to insulin sensitivity, lipolysis and GLP-1 concentrations in humans*. Sci Rep, 2019. **9**(1): p. 12515.
168. Fernandes, J., et al., *Adiposity, gut microbiota and faecal short chain fatty acids are linked in adult humans*. Nutr Diabetes, 2014. **4**(6): p. e121.
169. Brown, A.J., S. Jupe, and C.P. Briscoe, *A family of fatty acid binding receptors*. DNA Cell Biol, 2005. **24**(1): p. 54-61.
170. Kinouchi, K., et al., *Fasting Imparts a Switch to Alternative Daily Pathways in Liver and Muscle*. Cell Rep, 2018. **25**(12): p. 3299-3314 e6.

171. Zhang, F., et al., *Gene Expression Profile Change and Associated Physiological and Pathological Effects in Mouse Liver Induced by Fasting and Refeeding*. PLOS ONE, 2011. **6**(11): p. e27553.
172. Zhang, T., et al., *Akkermansia muciniphila is a promising probiotic*. Microb Biotechnol, 2019. **12**(6): p. 1109-1125.
173. Taoka, Y., et al., *Use of live and dead probiotic cells in tilapia Oreochromis niloticus*. Fisheries Science, 2006. **72**(4): p. 755-766.

ABSTRACT**THE PROBIOTIC EFFECT OF *CLOSTRIDIUM COCHLEARIUM* IS ASSOCIATED WITH SIGNIFICANT CHANGE OF SHORT-CHAIN FATTY ACID METABOLISM AND GUT MICROBIOTA**

by

QING AI**August 2021****Advisor:** Dr. Kequan Zhou**Major:** Nutrition and Food Science**Degree:** Doctor of Philosophy

The prevalence of obesity is rising steadily across the world, which increases the risk of many metabolic diseases and life-threatening illnesses. A specific strain, *Clostridium cochlearium* (*C. cochlearium*), reported as a butyrate producer, could have potential probiotic effects against obesity. The objective of this study was to evaluate the effects of dietary supplementation of *C. cochlearium* on a high-fat diet-induced obese (DIO) mouse model. The 16S rRNA sequencing of mice gut microbiome was performed at the end of the experimental period to identify the changes in gut microbial composition, investigate possible functional genes, and elucidate potential mechanisms. Thirty-six C57BL/6 6-8 week old male mice were randomly separated into three groups (n = 12): low-fat diet control (LF) group, high-fat diet control (HF) group, and experimental group on a high-fat diet with *C. cochlearium* supplementation (CC). After 16 weeks of dietary supplementation, the results showed the CC group had a 17.29% body weight reduction relative to the HF group ($P < 0.0001$), while 20.82% of fat mass decrease was observed compared to the HF group ($P < 0.0001$). The AUC of OGTT and HOMA-IR in the CC group was significantly reduced by 60.20% ($P < 0.0001$), 47.21% ($P < 0.01$), respectively. Moreover, the resting energy

expenditure ($P < 0.05$) and activity level ($P < 0.05$) showed a significant increase in the CC group. After performing alpha-and beta-diversity analyses, significant separation of the gut microbiome profile was observed between the HF and CC groups, which suggested the alteration of microbial compositions from the *C. cochlearium* supplementation. Additionally, the ratio of Firmicutes and Bacteroidetes (F/B) was significantly lower in the CC group compared to the HF group ($P < 0.05$). The family of *Ruminococcaceae* and *Lachnospiraceae*, as short-chain fatty acids (SCFAs) producers, significantly contributed to the gut community of the CC mice, which has been negatively associated with body weight. There was an increasing abundance of butyrate-producing enzymes and pathways observed from the CC group, which suggested a possible beneficial effect of a negative correlation with body weight gain. This study concluded that the administration of *C. cochlearium* had anti-obesity effects on reduced body weight gain and improve glucose homeostasis in the high-fat diet-induced obesity mouse model, which could be mediated through an increased abundance of SCFAs-producing bacteria and their related pathways. However, the butyrate ($P < 0.0001$) and acetate ($P < 0.001$) concentrations in the intestinal content showed a significant reduction in the CC group, which was unexpected and warranted further investigation of circulating SCFAs levels. This additional information may enhance our understanding of the probiotic effects of *C. cochlearium* supplementation.

AUTOBIOGRAPHICAL STATEMENT

Qing Ai

EDUCATION:

Wayne State University, Detroit, MI, US

Ph.D. in Nutrition and Food Science

Sep 2017 – Jul 2021

M.P.H. in Family Medicine & Public Health Sciences

Sep 2018 – Aug 2020

M.S. in Nutrition and Food Science

Sep 2015 – May 2017

Shanghai Business School, China

B.S. in Food Quality & Safety

Sep 2010 – Jul 2014

PROFESSIONAL EXPERIENCE:

- **Graduate Teaching Assistant**, Wayne State University, US Jan 2018 – May 2021
- **Graduate Research Assistant**, Wayne State University, US Jan 2016 – June 2021
- **Student Intern**, Detroit Health Department, US Jan 2020 – Apr 2020
- **Research Assistant**, Shanghai Institute of Planned Parenthood Research, China
Oct 2013 – Apr 2014
- **Student Intern**, Shanghai Food & Drug Administration, China Mar 2013 – Apr 2013
- **Student Intern**, Wuhu Food & Drug Administration, China Jan 2013

PUBLICATIONS:

- Yang, F., Zhu, W., Sun, S., **Ai, Q.**, Edirisuriya, P., & Zhou, K. (2020). *Isolation and Structural Characterization of Specific Bacterial β -Glucuronidase Inhibitors from Noni (*Morinda citrifolia*) Fruits. Journal of natural products*, 83(4), 825–833.
<https://doi.org/10.1021/acs.jnatprod.9b00279>
- **Ai Qing**, Wen Xue. (Sep 2013). *Development of Kudzu Vine Root Colorful Noodle. Anhui Province Economy*, 09/24/2013, P.10.
- Lu Wenwei, Huang Yue, **Ai Qing**, Bai Chen. (July 2013). *Determination of acrylamide in Moon cake by High Performance Liquid Chromatography. Food Research & Development*, 7/2013, 92-93

PROFESSIONAL AWARDS AND CERTIFICATES

- **Graduate Teaching Assistantship**, Wayne State University, US Jan 2018 – May 2021
- **Responsible Conduct of Research (RCR)**, Wayne State University May 2018
- **Research Assistantship**, Wayne State University, US Jun 2017 – Dec 2017
- **Animal Handling Training**, CITI-Wayne State University Jan 2017
- **Introductory of HACCP course**, Wayne State University Jul 2016
- **Graduate Professional Scholarship**, Wayne State University, US Aug 2015 – Apr 2016